KADIR HAS UNIVERSITY
SCHOOL OF GRADUATE STUDIES
DEPARTMENT OF ENGINEERING AND NATURAL SCIENCES

THE EFFECT OF LINK MODIFICATIONS ON NETWORK SYNCHRONIZATION

NARÇİÇEĞİ KIRAN

MASTER OF SCIENCE THESIS

ISTANBUL, JUNE, 2022

THE EFFECT OF LINK MODIFICATIONS ON NETWORK SYNCHRONIZATION

NARÇİÇEĞİ KIRAN

A thesis submitted to
the School of Graduate Studies of Kadir Has University
in partial fulfilment of the requirements for the degree of
Master of Science in
Computational Applied Science and Engineering

Istanbul, June, 2022

APPROVAL

This thesis titled THE EFFECT OF LINK MODIFICATIONS ON NETWORK SYNCHRONIZATION submitted by NARÇİÇEĞİ KIRAN, in partial fulfillment of the requirements for the degree of Master of Science in Computational Applied Science and Engineering is approved by

Asst. Prof. Dr. Deniz Eroğlu (Advisor) .....
Kadir Has University

Prof. Dr. Ayşe Hümeyra Bilge .....
Kadir Has University

Assoc. Prof. Dr. Şükrü Yalçınkaya .....
Istanbul University

I confirm that the signatures above belong to the aforementioned faculty members.

.....
Prof. Dr. Mehmet Timur Aydemir
Director of School of Graduate Studies
Date of Approval: 20.06.2022

DECLARATION ON RESEARCH ETHICS AND PUBLISHING METHODS

I, NARÇİÇEĞİ KIRAN; hereby declare

- that this Master of Science Thesis that I have submitted is entirely my own work and I have cited and referenced all material and results that are not my own in accordance with the rules;
- that this Master of Science Thesis does not contain any material from any research submitted or accepted to obtain a degree or diploma at another educational institution;
- and that I commit and undertake to follow the "Kadir Has University Academic Codes and Conduct" prepared in accordance with the "Higher Education Council Codes of Conduct".

In addition, I acknowledge that any claim of irregularity that may arise in relation to this work will result in a disciplinary action in accordance with university legislation.

NARÇİÇEĞİ KIRAN

.....

20.06.2022

ACKNOWLEDGEMENT

Firstly, I want to thank my advisor and the founder of the Nodds Lab Asst. Prof. Dr. Deniz Eroğlu, for his guidance, encouragement, and continuous support, started the day I met him. He did everything to make a sustainable and genuine scientific environment and supported me with his invaluable information, knowledge, and feedback. Also, I want to thank Prof. Tiago Pereira, who has shared his expertise and information with us throughout the project. My sincere gratitude goes to Sajjad Bakrani for providing further discussions and contributing significantly to the analytical aspects of this research. Furthermore, I thank the members of the Nodds Lab for being on my side despite the pandemic and giving me the joy of solidarity.

I would like to acknowledge and thank the Scientific and Technological Research Council of Turkey (TUBITAK) and BIDEB for my scholarship under the 2232 Grant No. 118C236. I would also like to thank Kadir Has University for the full scholarship and additional financial life support.

Last but not least, I am thankful to my mother, Nefise Sormageç, for inspiring me with her patience and kindness.

THE EFFECT OF LINK MODIFICATIONS ON NETWORK SYNCHRONIZATION

ABSTRACT

A major issue in studying complex network systems, such as neuroscience and power grids, is understanding the response of network dynamics to link modifications. The notion of network $\mathcal{G}(G, f, H)$ refers to diffusively coupled identical oscillators, where isolated dynamics are chosen to be chaotic. As a consequence of the diffusive nature, a globally synchronized state emerges as an invariant synchronization subspace, and it will be locally stable above critical coupling strength. Furthermore, the real part of the second minimum eigenvalue of the Laplacian matrix is inverse proportional to the critical coupling strength. Thus, we can use it to determine the synchronizability between two networks. Due to the asymmetry of the Laplacian matrix of a directed graph, adding directed links might cause a decrease in the real part of the second minimum eigenvalue of the Laplacian. If, after adding a link to a graph in a given network, the real part of the second minimum eigenvalue of the Laplacian matrix increases, it is called the enhancement of synchronization. Otherwise, it is called the hindrance of synchronization. In this research, we explore how the stability of synchronization at diffusively coupled oscillators is affected by link modifications for the networks created using particular motifs, i.e., cycle and star motifs. We consider a weakly connected directed graph consisting of two strongly connected components connected by directed link(s) (called cutset). We study the synchronization transitions in such networks when new directed link(s) between the components, in the opposite direction of the cutset, is added and strongly connects the whole network. We explore which properties of underlying graphs and their connected components may hinder or enhance the synchronization.

Keywords: Laplacian matrix, spectral gap, Braess's paradox, eigenvalue perturbation, network perturbation

ÖZET

Nörobilim ve güç şebekeleri gibi karmaşık ağ sistemlerini çalışırken, ağ senkronizasyonun kenar değişikliklerine tepkisini anlamak oldukça önemlidir. $\mathcal{G}(G, f, H)$ ağı kavramı, bu araştırma boyunca difüzyon ile yayılan, kuple olmuş, özdeş ve izole dinamikleri kaotik seçilmiş salınıcılara (osilatör) atıfta bulunur. Difüzyonun doğası gereği, global olarak senkronize durumda, değişmez bir senkronizasyon alt uzayı ortaya çıkar ve bu senkronize durum, etkileşme sabiti kritik değerin üzerinde iken yerel olarak kararlıdır. Ayrıca, Laplasyen matrisinin ikinci minimum özdeğerinin gerçek kısmı, kritik etkileşme kuvvetiyle ters orantılıdır. Böylece, onu iki ağ arasındaki senkronizasyonu belirlemek için kullanabiliriz. Yönlü bir çizgenin Laplasyen matrisinin asimetrisi nedeniyle, yönlü bağlantıların eklenmesi, Laplasyen matrisinin ikinci minimum özdeğerinin gerçek kısmında bir azalmaya neden olabilir. Belirli bir ağdaki bir çizgeye bir bağlantı eklendikten sonra, Laplasyen matrisinin ikinci minimum özdeğerinin gerçek kısmı artarsa, buna senkronizasyonun iyileştirilmesi denir. Aksi takdirde, senkronizasyon engeli olarak adlandırılır. Bu araştırmada, belirli motifler, yani halka ve yıldız motifleri kullanılarak oluşturulan ağlar için bağlantı modifikasyonlarından, difüzyonla yayılan, kuple olmuş, özdeş salınıcılarda senkronizasyon kararlılığının nasıl etkilendiğini araştırıyoruz. Yönlü kenar(lar) (kesme olarak adlandırılır) ile birbirine bağlanan, güçlü şekilde bağlı iki bileşenden oluşan zayıf bağlantılı yönlü çizgeleri ele alıyoruz. Bu tür ağlardaki senkronizasyon geçişlerini, kesme setinin zıt yönünde bileşenler arasında yeni yönlü kenar(lar) eklendiğinde ve tüm ağı güçlü bir şekilde bağladığında inceliyoruz. Temel çizgelerin ve bunların bağlantılı bileşenlerinin hangi özelliklerinin senkronizasyonu engelleyebileceğini veya geliştirebileceğini araştırıyoruz.

Anahtar Sözcükler: Laplasyen matrisi, spektral aralık, Braess paradoksu, özdeğer pertürbasyonu, ağ pertürbasyonu

TABLE OF CONTENTS

LIST OF FIGURES

LIST OF SYMBOLS

$\mathbf{1}_k$	k-dimensional vector whose entries are all 1
A_{ij}	the element at the ith row and jth column of the adjacency matrix
C	Cutset matrix
C_n	a cycle graph on n vertices
$\mathbb{C}^n$	Complex n-space
$\mathcal{C}^r$ function	a function with r continuous derivatives
D	Differential operator
d_i	In-degree of a vertex i
δ_{ij}	Kronecker delta
Δ	Perturbation matrix
E	Synchronization error
f	Isolated dynamics
K_n	a complete graph on n vertices
$K_{n,m}$	a complete bipartite graph
L	Laplacian matrix
L_G	Unperturbed Laplacian matrix
L_{G_p}	Perturbed Laplacian matrix
M	Synchronization manifold
M_n	the set of $n \times n$ square matrices
G	a graph
H	Coupling function
P_n	a path on n vertices
S_m	a star graph on m vertices
Re	Real part
$\mathbb{R}^n$	n-dimensional Euclidean space
t	Time variable
$\forall$	the universal quantifier
$\exists$	the existential quantifier
λ_2	Spectral gap
$\square$	which was to be proven

Θ	Coupling strength
Θ_c	Critical coupling strength
$\mathcal{G}$	Network
$E(G)$	the edge set of G
$V(G)$	the vertex set of G
A^T	Transpose of A
$Disc(a_{ii}, R_i)$	a disc centered at a_{ii} with radius R_i
w_i	the weight of the edge i starting from cycle to star
δ_i	the weight of the edge i starting from star to cycle

LIST OF ACRONYMS AND ABBREVIATIONS

AC	Alternative Current
Digraph	Directed Graph
etc.	and so on
et al.	and others
e.g.	for example
i.e.	in other words
ODE	Ordinary Differential Equation

1. INTRODUCTION

1.1 Motivation

Complex systems consisting of coupled units appear in many fields ranging from neuroscience (Ermentrout and Terman, 2010, p. 241) to engineering (Newman, 2018, pp. 17-99). To analyze such systems, the first question that we can ask is how the single dynamical system works, e.g., isolated animal species, AC power generator, a neuron, and whose evolutions in time. Subsequently, how the whole system behaves when we take many such dynamical systems and allow them to interact with each other (Figure 1.1).

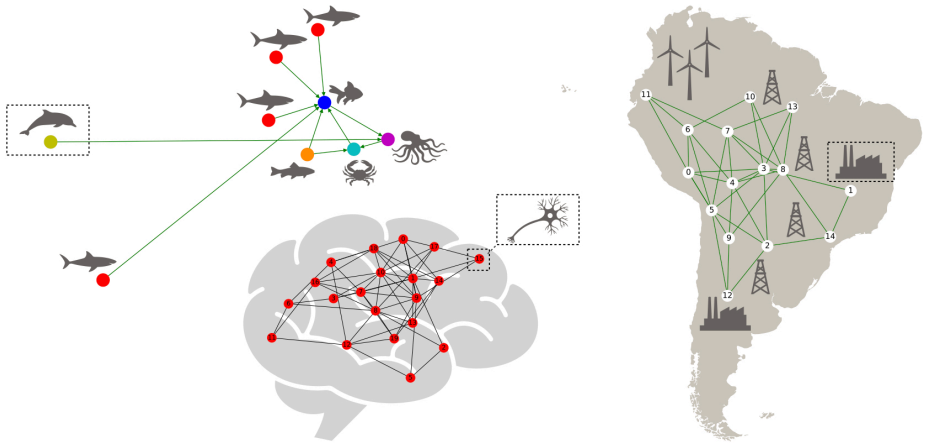

Figure 1.1: Real-world Examples of Complex Systems

We consider the network of dynamical systems. Hence, the notion of network $\mathcal{G}(G, f, H)$ refers to diffusively coupled identical oscillators throughout this survey, and it encapsulates the information of three components. The first component is the graph G. When a diffusion scheme forms the next state of a given oscillator using the difference between the current state and the input state, the underlying graph structure dictates the input states, i.e., linked oscillators to the given oscillator. The second component is the isolated dynamics f. Each oscillator has identical behav-

ior, and isolated dynamics are chosen to be chaotic, meaning the small variations of oscillators' initial conditions cause the divergence of nearby trajectories. The last component is the coupling function H, which describes the functional aspects of interactions, i.e., the physical rule about how the interactions occur. Due to particular interest, the coupling function is chosen as identity, and the research is focused on structural aspects of interactions.

For such models, prey-predator dynamics might emerge from the competition in ecological networks, or to transmit a signal in power grids, the phases of alternating currents generated by different generators are required to act coherently in time. The emergent phenomenon when the units act coherently in time ("adjustment of rhythms due to an interaction" (Pikovsky, Rosenblum and Kurths, 2001, p. xviii).) is called synchronization. C. Huygens, a physicist, discovered this phenomenon during his works on pendulum clocks in the XVII century. Since then, the synchronization of networks and understanding the critical transitions between synchronization and desynchronization have become essential to interpret the processes encountered in basic science, technology, and engineering problems.

Although synchronization is a well-known subject now (Pikovsky, Rosenblum and Kurths, 2001, pp. 1-23), it still has many unexplained parts, such as the effects of topological revisions on the general structure of networks. For instance, perturbing a network by adding a new connection was assumed to increase the network's connectivity and consequently increase the network's synchronizability. Yet, a German mathematician Dietrich Braess discovered that this might not be true in general. The experiment discovered goes as follows: Suppose there exist two choices from 'start' to 'end,' namely road A and road B, as given in Figure 1.2. Let T denote the number of travelers that uses the road. Since both roads have equal time spent, the travelers are in equilibrium when road A and road B have 1000 travelers each. The total travel time is 30 minutes. Then, the orange-color junction is added to relax the traffic flow, as given in Figure 1.3. Travelers noticed that if they choose the $T/100$ roads merged by the junction, they will spend at most 20 minutes at each $T/100$ road. Thus, every traveler decides to use $T/100$ roads, and the total travel

time becomes 40 minutes. In conclusion, Braess's paradox states that adding one or more roads to a road network can slow down overall traffic flow (Braess, 1968, pp. 258-268).

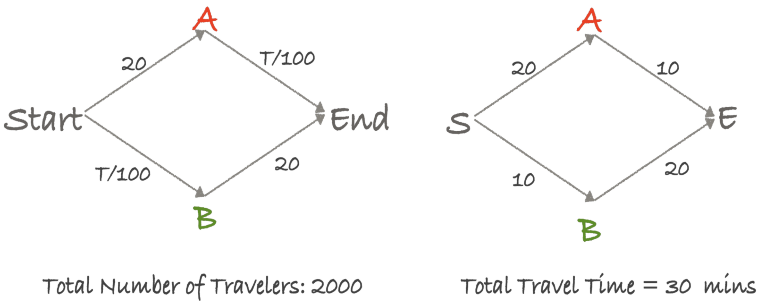

Figure 1.2: Braess's Paradox Before Modification

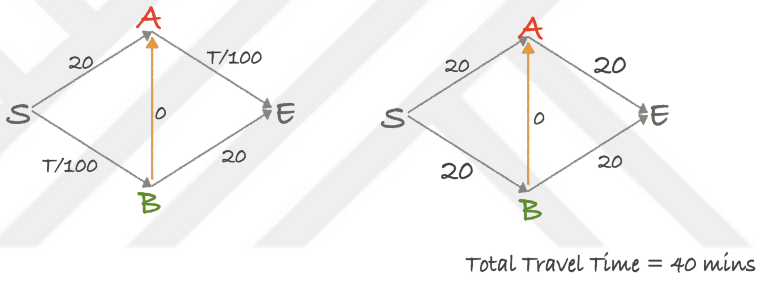

Figure 1.3: Braess's Paradox After Modification: When the orange road is added, the total travel time becomes 40 minutes.

Recently, it has been proved that some cases for directed networks exist such that improving the network structure may lead to functional failures similar to Braess's paradox (Poignard, Pade and Pereira, 2019, pp. 1919-1942). These functional failures present themselves in real life as the long-lasting synchronized firing during the neural activity, which may trigger an epilepsy crisis or the phase differences between alternating currents in power grids which may cause regional blackouts. Even though it is vital to determine when these functional failures occur exactly, there is still a lack of rigorous results due to the high complexity of such problems.

In this research, we explore how the stability of synchronization at diffusively coupled oscillators is affected by link modifications for the networks created using particular motifs, i.e., cycle and star motifs. There exists a comparison of the synchronizability

between two networks via their critical coupling strengths. The comparison will be reduced to the underlying graph structure if isolated dynamics and the coupling function are the same for such two networks. More precisely, the spectral properties of the Laplacian matrix (i.e., the real part of the second minimum eigenvalue of the Laplacian) representing the network determine the synchronizability between two networks. Moreover, the critical coupling strength is inverse proportional to the real part of the second minimum eigenvalue of the Laplacian matrix. Thus, if after adding a link to a graph in a given network, the real part of the second minimum eigenvalue of the Laplacian matrix increases, it is called the enhancement of synchronization. Otherwise, it is called the hindrance of synchronization. This research gives an exact prescription to see if a modification enhances or hinders the synchronization based on underlying graph parameters for the first time. It is unknown for now how much of these results can be generalized. Nevertheless, the prediction of stability transitions of the synchronization may help the sanation and control of the system's state before function loss and provides bases for the application of optimized modifications.

1.2 Literature Review and Contributions

In the past decades, research revealed that the interaction structure of the network plays a crucial role in the function of coupled dynamics (Eroglu, Lamb and Pereira, 2017, pp. 207-243). Such networks can be translated as a combination of certain motifs, such as trees or cycles, and these motifs dictate the dynamical behavior and provide the resilience of the overall system. Predicting the impact of the network structure on the dynamics is an intricate nonlinear problem that leads to many unexpected results. Indeed, in some situations improving the network structure may lead to functional failures, e.g., Braess's paradox (Eldan, Rácz and Schramm, 2017, pp. 584-611), and synchronization loss (Pade and Pereira, 2015, pp.1-6).

Many phenomena, including synchronization, random walks, and cascade failure, intrinsically depend on the spectral properties of the underlying graph. Thus, the problem resides first in understanding the spectral changes.

Although certain correlations between network structure and dynamics have been observed in experimental (Hart et al, 2015, p. 022804) and numerical investigations (Nishikawa and Motter, 2010, pp. 10342-10347), most of these results are concerned with small modifications to the network. Such as the addition of new links of small weights. There is a lack of rigorous results to determine the relationship between the network structure and its dynamic properties. Most of the results in this direction rely on the perturbation theory of eigenvalues to determine which structural changes are detrimental to the network dynamics.

Many interesting questions are clearly not uncovered via perturbation theory. In fact, previous results relying on perturbation theory suggest that desynchronizing the network by adding new links is unusual, and most perturbations would actually lead to better, more stable synchronization (Poignard, Pade and Pereira, 2019, pp. 1919-1942). To understand this problem, we need to unveil the full nonlinear picture and deal with large changes in the topology.

In this research, we will focus on an important motif generally appearing in complex networks. We will consider a cycle coupled with a star. Even if both motifs are typical and have a fully developed spectral theory by themselves (Brouwer and Haemers, 2011, pp.8-10), understanding their interaction and completely characterizing the spectrum when both are connected remains an open problem.

1.3 Organization

The sections of the thesis are organized as follows:

- **Chapter 2: Dynamical Systems**

  We give fundamental definitions of dynamical systems and introduce two examples of strange attractors, namely the Lorenz and Rössler Models.

- **Chapter 3: Synchronization**

  We discuss the local stability of global synchronization for two coupled systems and for $n-$dimensional diffusively coupled identical oscillators. Then, we present a comparison of synchronizability in complex networks via graphs' spectra.

- **Chapter 4: Graph Theory** We investigate some fundamentals of graph theory and revisit some spectral properties of a graph.
- **Chapter 5: Unexpected Emergent Behavior in Network Dynamics**
  We present our problem setting, i.e., the cycle-star motif, and state our graph-theoretical results. Then, we explore the synchronizability behavior of given networks generated by the cycle-star motif using the reduction of synchronizability in complex networks to the spectral properties of underlying graphs.
- **Chapter 6: Proofs of The Main Results**
  In Section 6.2, we discuss the techniques that are used in the proofs of the theorems. We then prove Theorem B in Section 6.3. Finally, we prove Theorem C in Section 6.4.
- **Chapter 7: Conclusions**
  We provide some informal results of our findings and state some open problems for further investigations.

2. DYNAMICAL SYSTEMS

In this section, we provide fundamental definitions of dynamical systems and introduce two examples of strange attractors, namely the Lorenz and Rössler Models.

2.1 Fundamental Definitions of Dynamical Systems

Definition 2.1.1. Consider $\mathbb{R}^n$ $(n \geq 0)$. Let $t \in \mathbb{R}$ and x be a point in $\mathbb{R}^n$. A **dynamical system** is a function

$$\begin{aligned} \phi :& \mathbb{R} \times \mathbb{R}^n \to \mathbb{R}^n \\ & (t, x) \mapsto \phi(t, x) \end{aligned} \tag{2.1}$$

that satisfies

- $\phi(0, x) = x$ for all $x \in \mathbb{R}^n$.
- $\phi(t_2, \phi(t_1, x)) = \phi(t_1 + t_2, x)$ for all $x \in \mathbb{R}^n$ and for $t_1, t_2 \in \mathbb{R}$.

Definition 2.1.2. The **orbit** or **trajectory** of x_0 is the set $\{\phi(t, x_0) : \quad t \in \mathbb{R}\}$. Let $t = t_0 \in \mathbb{R}$. In this case,

$$\begin{aligned} \phi :& \mathbb{R}^n \to \mathbb{R}^n \\ & x \mapsto \phi(t_0, x) \end{aligned} \tag{2.2}$$

Definition 2.1.3. When time variable t is fixed, the function ϕ is called **time-t map**. (Discretization of a continuous-time system.)

Definition 2.1.4. (Wiggins, Golubitsky, 2003, p. 28) Let $A \subset \mathbb{R}^n$, where $A \neq \emptyset$. Then, A is **invariant** with respect to ϕ if for every point in A, the entire orbit of x_0 lies in A, i.e., $\phi(t, x_0) \in A$ for all $t \in \mathbb{R}$.

Definition 2.1.5. $\dot{x} := \frac{dx}{dt} = f(x)$ is called the system of ordinary differential equations.

$$\begin{aligned}
\frac{dx_1(t)}{dt} &= f_1\left(x_1(t), x_2(t), \cdots, x_n(t)\right), \\
\frac{dx_2(t)}{dt} &= f_2\left(x_1(t), x_2(t), \cdots, x_n(t)\right), \\
&\vdots \qquad\qquad \vdots \qquad\qquad \vdots \\
\frac{dx_n(t)}{dt} &= f_n\left(x_1(t), x_2(t), \cdots, x_n(t)\right),
\end{aligned} \tag{2.3}$$

where

$$f\begin{pmatrix} x_1 \\ x_2 \\ \vdots \\ x_n \end{pmatrix} = \begin{pmatrix} f_1(x_1, x_2, \cdots, x_n) \\ f_2(x_1, x_2, \cdots, x_n) \\ \vdots \\ f_n(x_1, x_2, \cdots, x_n) \end{pmatrix}, \quad f_i : \mathbb{R}^n \to \mathbb{R}\ (i = 1, \cdots, n). \tag{2.4}$$

We consider the flow $\phi(t, x)$ generated by $\mathcal{C}^r$ $(r \geq 1)$ [1] autonoumous vector fields on $\mathbb{R}^n$,

$$\dot{x} := \frac{dx}{dt} = f(x), \tag{2.5}$$

and we assume that it exists for all $t > 0$. We also assume that there is a compact set $\Lambda \subset \mathbb{R}^n$ invariant under $\phi(t, x)$, i.e., $\phi(t, \Lambda) \subset \Lambda$ for all $t \in \mathbb{R}$. We have the following definitions.

Definition 2.1.6. (Wiggins, Golubitsky, 2003, p. 736) The flow $\phi(t, x)$ is said to have **sensitive dependence on initial conditions** on Λ if there exists $\epsilon > 0$ such that, for any $x \in \Lambda$ and any neighborhood U of x, there exists $y \in U$ and $t > 0$ such that $|\phi(t, x) - \phi(t, y)| > \epsilon$.

Definition 2.1.7. (Wiggins, Golubitsky, 2003, p. 107) A closed invariant set $A \subset \mathbb{R}^n$ is called an **attracting set** if there is a neighborhood U of A such that $\phi(t, U) \subset U$ and $\cap_{t>0}\phi(t, U) = A$ for all $t \geq 0$.

[1] If $f(x, t)$ is $\mathcal{C}^r$ $(r \geq 1)$ in x and t, then solutions through any $x_0 \in \mathbb{R}^n$ exist and are unique on some time interval. (Proof: Picard-Lindelöf Theorem (Hirsch, Smale and Devaney, 2013, pp. 385-294))

Definition 2.1.8. (Wiggins, Golubitsky, 2003, p. 108) A positive invariant compact subset $B \subset \mathbb{R}^n$ is called an **absorbing set** if there exist a bounded subset U of $\mathbb{R}^n$ with $B \subset U$ and $t_U > 0$ such that $\phi(t, U) \subset B$ for all $t \geq t_U$.

Definition 2.1.9. (Wiggins, Golubitsky, 2003, p. 110) A closed invariant set A is said to be **topologically transitive** if, for any two open sets $U, V \subset A$, there exists $t \in \mathbb{R}$ such that $\phi(t, U) \cap V \neq \emptyset$.

Definition 2.1.10. An **attractor** is a topologically transitive attracting set.

Definition 2.1.11. (Wiggins, Golubitsky, 2003, p. 736) Λ is said to be **chaotic** if

(i) $\phi(t, x)$ has sensitive dependence on initial conditions on Λ.

(ii) $\phi(t, x)$ is topologically transitive on Λ.

Consider the $\mathcal{C}^r$ $(r \geq 1)$ vector field

$$\dot{x} = f(x),\ x \in \mathbb{R}^n \tag{2.6}$$

Let $x(t, x_0)$ be a trajectory of equation (2.6) satisfying $x(0, x_0) = x_0$. Consider the orbit structure of the linearization of equation (2.6) about $x(t, x_0)$ given by

$$\dot{\xi} = Df(x(t))\xi, \quad \xi \in \mathbb{R}^n. \tag{2.7}$$

Let $X(t; x(t, x_0))$ be the fundamental solution matrix of Eq. (2.7) and let $e \neq 0$ be a vector in $\mathbb{R}^n$. Then the coefficient of expansion in the direction e along the trajectory through x_0 is defined to be

$$\begin{aligned} \lambda_t(x_0, e) &= \frac{\|X(t; x(t, x_0))e\|}{\|e\|}, \\ &\text{where } \|.\| = \sqrt{\langle ., . \rangle}. \end{aligned} \tag{2.8}$$

Definition 2.1.12. (Wiggins, Golubitsky, 2003, p. 726) **The Lyapunov exponent** in the direction e along the trajectory through x_0 is

$$\chi(X(t; x_0(t, x_0)), x_0, e) = \lim_{t \to \infty} \frac{1}{t} \log \lambda_t(x_0, e) \tag{2.9}$$

Definition 2.1.13. A chaotic orbit is a bounded aperiodic orbit that has at least one positive Lyapunov exponent. (We define the Lyapunov exponent of a flow as the Lyapunov exponent of its time-T map for $T = 1$.)

Definition 2.1.14. (Wiggins, Golubitsky, 2003, p. 740) Suppose $A \subset \mathbb{R}^n$ is an attractor. Then A is called a **strange attractor** if it is chaotic.

Theorem 2.1.15. (Pereira, 2011, p. 43) Let B be a compact subset of the open set U. Consider Equation (2.6) and let f be differentiable. Let $x_0 \in B$ and suppose that every solution $x : [0, \tau] \to U$ with $x(0) = x_0$ lies entirely in B. Then this solution is defined for all (forward) time $t \geq 0$.

2.2 Two Famous Examples of Strange Attractors

Tucker introduced a computer-assisted proof of the existence of a strange attractor for the Lorenz model in 1999 (Tucker, 1999, pp. 1197-1202). Still, showing a dynamical system to possess a strange attractor is rather compelling. Instead, let us show the chaotic behavior of orbits when the model has at least one positive Lyapunov exponent.

2.2.1 Lorenz model

Edward Lorenz introduced the Lorenz model in 1963 to model atmospheric convection as follows:

$$\begin{aligned} \dot{x} &= \sigma(y - x) \\ \dot{y} &= x(\gamma - z) - y \\ \dot{z} &= -\beta z + xy \end{aligned} \tag{2.10}$$

where σ, γ, and β are real positive parameters of the system.

When parameters are selected as $\sigma = 10$, $\gamma = 28$, and $\beta = 8/3$, the model has sensitive dependence on initial conditions, i.e., the model has at least one positive Lyapunov exponent as shown in Figure (2.1), (2.2). The maximum Lyapunov exponent is found as $\chi_{max} \approx 0.9$ for these parameters.

On the other hand, when all Lyapunov exponents are negative in the model where $\sigma = 5$, $\gamma = 28$, $\beta = 8/3$, a fixed point occurs as shown in Figure 2.3.

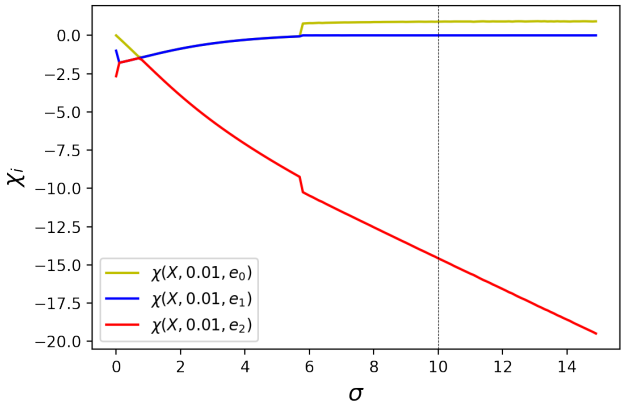

Figure 2.1: Lyapunov exponents of Lorenz model for varying σ where $\gamma = 28$ and $\beta = 8/3$. When $\sigma = 10$, the maximum Lyapunov exponent is $\chi_{max} \approx 0.9$.

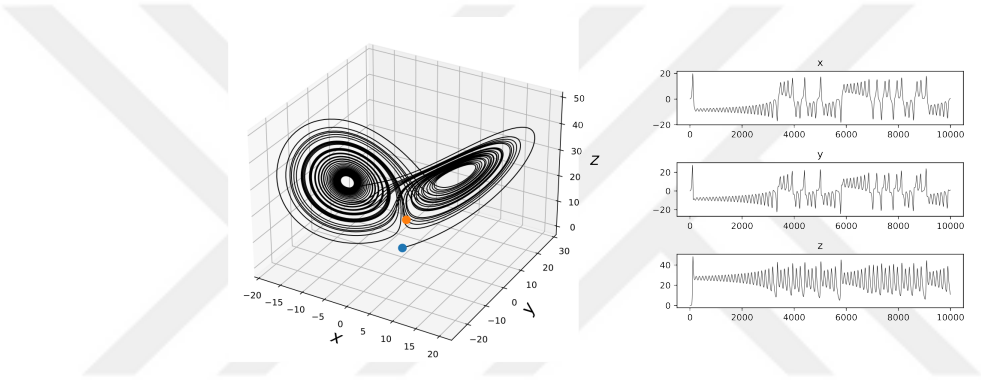

Figure 2.2: A chaotic trajectory of Lorenz model where $\sigma = 10$, $\gamma = 28$, $\beta = 8/3$ and $x_0 = 0.1, y_0 = 0.1, z_0 = 0.1$. Blue-color corresponds to the initial point, orange-color corresponds to the final point.

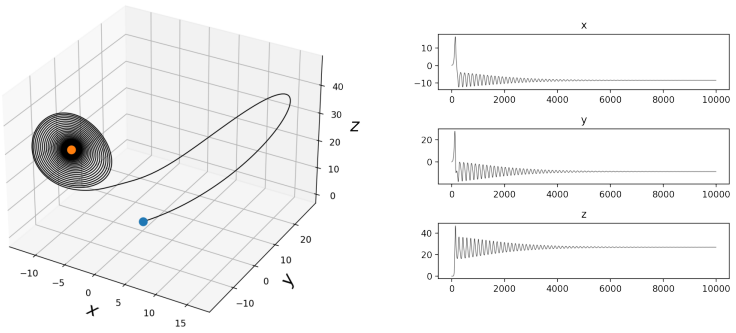

Figure 2.3: A fixed point in Lorenz model where $\sigma = 5$, $\gamma = 28$, $\beta = 8/3$ and $x_0 = 0.1, y_0 = 0.1, z_0 = 0.1$. Blue-color corresponds to the initial point, orange-color corresponds to the final point.

2.2.2 Rössler model

Otto Rössler introduced the Rössler model in 1976 as follows:

$$\begin{aligned} \dot{x} &= y - z \\ \dot{y} &= x + ay \\ \dot{z} &= b + z(x - c) \end{aligned} \tag{2.11}$$

where a, b, and c are real positive parameters of the system.

When parameters are selected as $a = 0.2$, $b = 0.2$, and $c = 5.7$, the model has sensitive dependence on initial conditions, i.e., the model has at least one positive Lyapunov exponent as shown in Figure (2.4), (2.5). The maximum Lyapunov exponent is found as $\chi_{max} \approx 0.07$ for these parameters.

On the other hand, when all Lyapunov exponents are negative in the model where $a = 0.2$, $b = 0.2$, $c = 4$, a periodic orbit occurs as shown in Figure 2.6.

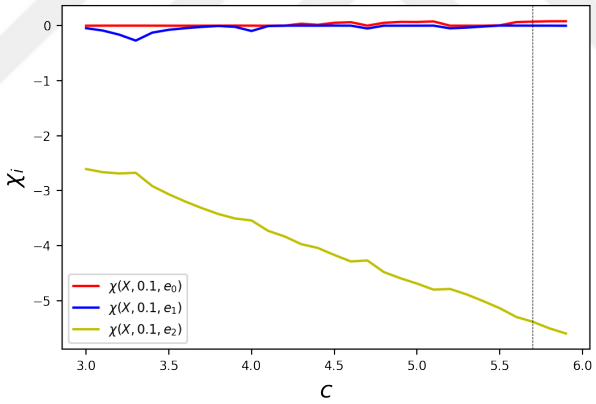

Figure 2.4: Lyapunov Exponents of Rössler Model for varying c where $a = 0.2$ and $b = 0.2$. When $c = 5.7$, the maximum Lyapunov exponent is $\chi_{max} \approx 0.07$.

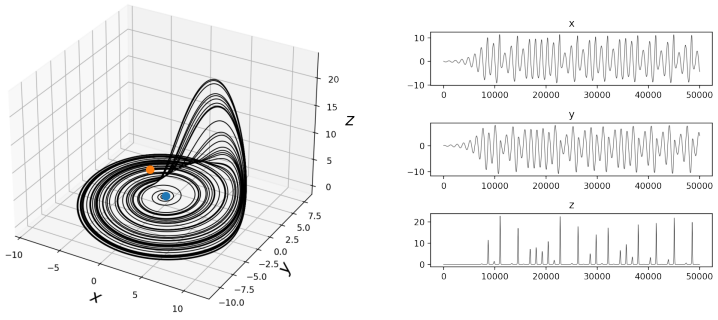

Figure 2.5: A trajectory for Rössler Model where $a = 0.2$, $b = 0.2$, $c = 5.7$ and $x_0 = 0.1, y_0 = 0.1, z_0 = 0.1$. Blue-color corresponds to the initial point, orange-color corresponds to the final point.

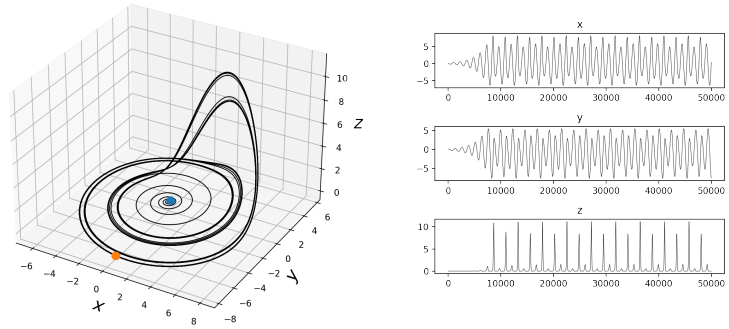

Figure 2.6: A periodic orbit in Rössler model where $a = 0.2$, $b = 0.2$, $c = 4$ and $x_0 = 0.1, y_0 = 0.1, z_0 = 0.1$. Blue-color corresponds to the initial point, orange-color corresponds to the final point.

3. SYNCHRONIZATION

In this section, we discuss the local stability of global synchronization for two coupled systems and generalize it to $n-$dimensional diffusively coupled identical oscillators. Then, we present a comparison of synchronizability in complex networks via graphs' spectra. Thus, we reduce the problem of synchronizability in complex networks to the spectral analysis of underlying graphs. We omitted some basic definitions of graph theory to preserve the continuity of the topic but we present them in detail in the next section. Note that, we briefly refer complete synchronization as synchronization throughout this chapter.

3.1 Synchronization Between Two Coupled Systems

We consider two fully diffusively coupled identical m-dimensional systems

$$\begin{aligned} \dot{x}_1 &= f(x_1) + \Theta H(x_2 - x_1) \\ \dot{x}_2 &= f(x_2) + \Theta H(x_1 - x_2) \end{aligned} \tag{3.1}$$

where $f : \mathbb{R}^m \to \mathbb{R}^m$ is the isolated dynamics, Θ is the overall coupling strength, $H : \mathbb{R}^m \to \mathbb{R}^m$ is the generalized coupling function. We set $H(0) = 0$ in order to generate the synchronization subspace such that $x_1 = x_2$ is invariant for all coupling strengths Θ. Note that, the diffusive coupling term vanishes for non-trivial coupling strengths and the system behaves as if the overall coupling strength $\Theta = 0$.

We will show the locally asymptotic stability of globally synchronized state, i.e.,

$$\begin{aligned} \lim_{t\to\infty} \|\mathbf{x}_1(t) - \mathbf{x}_2(t)\| = 0, \\ \text{where } \|.\| = \sqrt{\langle ., . \rangle}, \end{aligned} \tag{3.2}$$

for sufficiently strong coupling strengths Θ. Suppose coupling function is identity operator, i.e., $H = I$. We define the difference variable $z := x_1 - x_2$. Thus,

$$\begin{aligned} \dot{z} =& \dot{x}_1 - \dot{x}_2 \\ =& f(x_1) - f(x_2) - 2\Theta z \end{aligned} \tag{3.3}$$

Using Taylor expansion near $x_1 = x_2$, we get

$$\begin{aligned} f(x_2(t)) =& f(x_1(t)) - Df(x_1(t))(x_2(t) - x_1(t)) \\ &+ O(\|x_1(t) - x_2(t)\|^2) \\ f(x_2(t)) =& f(x_1(t)) - Df(x_1(t))z(t) + O(\|z(t)\|^2) \end{aligned} \tag{3.4}$$

where $Df(x_1(t))$ is the Jacobian matrix of $f(x)$ at $x_1(t)$. Thus,

$$\frac{dz}{dt} = [Df(x_1(t)) - 2\Theta I]z + O(\|z\|^2). \tag{3.5}$$

When we exclude the term $O(\|z\|^2)$ in equation (3.5), we call this expression as the first variational equation. If we introduce a new variable

$$\omega(t) = e^{2\Theta t}z(t) \tag{3.6}$$

then,

$$\begin{aligned} \dot{\omega}(t) &= 2\Theta e^{2\Theta t}z(t) + e^{2\Theta t}\dot{z}(t) \\ &= 2\Theta\omega[Df(x_1(t)) - 2\Theta I]e^{2\Theta t}z \\ &= [Df(x_1(t))]w \end{aligned} \tag{3.7}$$

Let $\phi(x_1(t))$ be the fundamental matrix for the variational equation, then any solution to the system may be described by $z(t) = \phi(x_1(t))z(0)$.

Let Λ be the maximal Lyapunov exponent of the orbit $x_1(t)$. Then,

$$\|\omega(t)\| \leq Ce^{\Lambda t}, \text{ for some constant } C > 0. \tag{3.8}$$

Since $\omega(t) = e^{2\Theta t}z(t)$, it follows that

$$\|z(t)\| \leq Ce^{(\Lambda - 2\Theta)t} \tag{3.9}$$

and thus,

$$\Theta_c = \frac{\Lambda}{2} \tag{3.10}$$

which implies that it is possible to determine the critical coupling using the maximal Lyapunov exponent of the system and if the system has $\Theta > \Theta_c$, synchronization is stable under small perturbations (Eroglu, Lamb and Pereira, 2017, pp. 207-243).

3.2 Network Dynamics

Henceforward, we can set a network, nodes of which are n identical oscillators, and their individual equation of motion corresponds to the dissipative dynamical system.

Let the network of these oscillators interact through a diffusive coupling that is proportional to the difference of state vectors $x_j(t) - x_i(t)$, where i, j represent the nodes of the network.

We consider a triplet $\mathcal{G} = (G, f, H)$, where G is a weighted digraph (discussed in details in Section 4), and $f, H \in \mathcal{C}^1(\mathbb{R}^l)$ for $l \geq 1$. The triplet $\mathcal{G}$ defines a system of ODEs of the form

$$\dot{x}_i = f(x_i) + \Theta \sum_{j=1}^{N} A_{ij} H(x_j - x_i), \qquad i = 1, 2, \ldots, N, \tag{3.11}$$

where $\Theta \geq 0$ is called the coupling strength. Each variable x_i represents a node of the graph G, the function f describes the isolated dynamics at each node, and the function H, called the coupling function. We call the triplet $\mathcal{G}$ or its associated system of ODEs (3.11) a network of diffusively coupled (identical) systems.

3.3 Synchronization in Complex Networks

The interaction term in equation (3.11) can be written in terms of Laplacian matrix L.

$$\begin{aligned}
\sum_{j=1}^{n} A_{ij}[H(x_j) - H(x_i)] &= \sum_{j=1}^{n} A_{ij} H(x_j) - H(x_i) \sum_{j=1}^{n} A_{ij} \\
&= \sum_{j=1}^{n} A_{ij} H(x_j) - d_i H(x_i) \\
&= \sum_{j=1}^{n} (A_{ij} - \delta_{ij} d_i) H(x_j)
\end{aligned}$$

where $d_i = \sum_{ij}^{n} A_{ij}$ is the in-degree of the ith node, δ_{ij} is the Kronecker delta, and $L_{ij} = \delta_{ij} d_i - A_{ij}$. Therefore, equation (3.11) is equivalent to the following form

$$\dot{x}_i = f(x_i) - \Theta \sum_{j=1}^{n} L_{ij} H(x_j), \tag{3.12}$$

where $\sum_j L_{ij} = 0$.

We define the synchronization manifold as

$$M := \{(x_1, \ldots, x_N) : \quad x_1 = \cdots = x_N \in U\}. \tag{3.13}$$

We say a network $\mathcal{G}$ synchronizes if there exists an open neighborhood $V \subseteq \mathbb{R}^{Nl}$ of M such that the forward orbit of any point in V converges to M. In other words, the synchronization manifold attracts its nearby orbits. It is shown (Pereira et al, 2014, pp. 501-525) that for a network $\mathcal{G}$ with a coupling strength Θ, if

1. The graph G has a spanning diverging tree (see 4.2.8).
2. There exists an inflowing open ball $U \subset \mathbb{R}^l$ which is invariant with respect to the flow of the isolated system $\dot{x} = f(x)$, and we have $\|Df(x)\| \leq K$ for some $K > 0$ and for all $x \in U$.
3. We have $H(0) = 0$. Moreover, all the eigenvalues of $DH(0)$ are real and positive.

then there exists $\Theta_c \geq 0$ such that when $\Theta \geq \Theta_c$, $\mathcal{G}$ synchronizes. We call Θ_c the critical coupling strength. It is given by

$$\Theta_c = \frac{\rho}{\beta \mathrm{Re}(\lambda_2)}, \tag{3.14}$$

where λ_2 is the second minimum eigenvalue of the Laplacian matrix, $\rho = \rho(f, DH(0))$ and $\beta := \min \sigma\left(DH\left(0\right)\right)$ are constants which only depend on f and/or $DH(0)$.

Equation (3.14) with assumptions stated above gives us a criterion to compare synchronizability in networks. More precisely, we have the following definition.

Definition 3.3.1. Consider two networks $\mathcal{G}_1 = (G_1, f_1, H_1)$ and $\mathcal{G}_2 = (G_2, f_2, H_2)$ that satisfy the assumptions above. Let $\Theta_c(\mathcal{G}_1)$ and $\Theta_c(\mathcal{G}_2)$ be the critical coupling strengths of $\mathcal{G}_1$ and $\mathcal{G}_2$, respectively. We say $\mathcal{G}_1$ is more synchronizable than $\mathcal{G}_2$ if $\Theta_c(\mathcal{G}_1) < \Theta_c(\mathcal{G}_2)$.

Having $\Theta_c(\mathcal{G}_1) < \Theta_c(\mathcal{G}_2)$ means that $\mathcal{G}_1$ synchronizes for a larger range of Θ than $\mathcal{G}_2$. Let us now consider the case that two networks $\mathcal{G}_1$ and $\mathcal{G}_2$ only differ in their topology, i.e. having the same isolated dynamics and coupling functions while the graph structures can be different. In this case, following equation (3.14), the second

minimum Laplacian eigenvalue of the underlying graphs of the networks determine which one is more synchronizable. Indeed, let consider two networks $\mathcal{G}_1 = (G_1, f, H)$ and $\mathcal{G}_2 = (G_2, f, H)$ that satisfy the assumptions above. Moreover, let $\lambda_2(G_1)$ and $\lambda_2(G_2)$ be the second minimum eigenvalues of G_1 and G_2, respectively. Then, the network $\mathcal{G}_1$ is more synchronizable than $\mathcal{G}_2$ if and only if $\lambda_2(G_1) > \lambda_2(G_2)$.

Before discussing our results of synchronization in networks with cycle-star motifs, we present some results in graph theory in the next section.

4. GRAPH THEORY

Graph theory surveys the diagrammatic abstraction of the pairwise relations between units (Figure 4.1). Graphs and their spectral properties provide general models and results applicable to diverse real-world systems. In this section, we investigate some fundamentals of graph theory, present our models and discuss how the perturbation, i.e., link addition(s), affects these models.

4.1 Basic Definitions and Matrices Associated to a Graph

Definition 4.1.1. (Bondy and Murty, 1976, p. 2; West, 2001, p. 2) A **graph** G is a triple (V, E, ψ_G) consisting of a vertex set $V(G)$, an edge set $E(G)$, and the incidence function $\psi_G : E \to V^{(2)}$ that associates with each edge of G two vertices (not necessarily distinct) of G .

Example 4.1.2.

The graph H as a triple:

$$V(H) = \{v_1, v_2, v_3, v_4\}$$
$$E(H) = \{e_1, e_2, e_3, e_4, e_5, e_6\}$$
$$\psi_G(e_1) = \{v_1, v_2\}$$
$$\psi_G(e_2) = \{v_1, v_2\}$$
$$\psi_G(e_3) = \{v_2, v_3\}$$
$$\psi_G(e_4) = \{v_3, v_3\}$$
$$\psi_G(e_5) = \{v_3, v_4\}$$
$$\psi_G(e_6) = \{v_4, v_1\}$$

The graph H as a diagram:

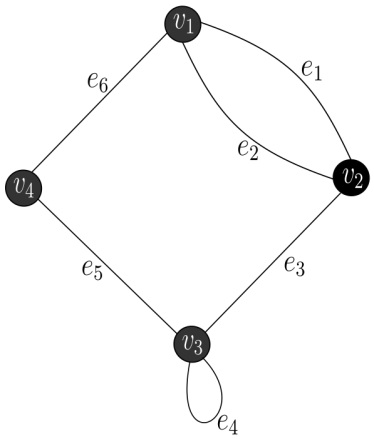

Figure 4.1: The graph H

Definition 4.1.3. (Bondy and Murty, 1976, p. 3) An edge with identical ends is called a **loop**, and an edge with distinct ends is called **link**. Two or more links with the same pair of ends are said to be **parallel edges**.

Definition 4.1.4. (Bondy and Murty, 1976, p. 3) A graph G is called **simple** if it has no loops or parallel edges (ψ_G is an injection of E into the set of subsets in V). (See Figure 4.2).

In this study, simple graphs are considered where mention of ψ_G is omitted, and the edges are viewed as a set of subsets of V with two elements. Thus, the graph G is defined as $G = (V, E)$ where $V = \{v_1, \ldots, v_n \,|\, n$ is the number of vertices$\}$ is the vertex set and $E = \{e_1, \ldots, e_n\} \subset V \times V$ is the edge set.

Definition 4.1.5. A **directed graph**, also called a digraph, $G = (V, E)$ consist of vertices and ordered pairs of edges such that the pair $e_k = (i, j) \in E$ represents the kth edge directed from vertex j (the tail of e_k) to vertex i (the head of e_k) and an edge may also have a weight w associated with it.

Definition 4.1.6. The graph is called **undirected** if the edge set is not ordered ($E \subset V \times V$ such that $(i, j) \in E$ if and only if $(j, i) \in E$).

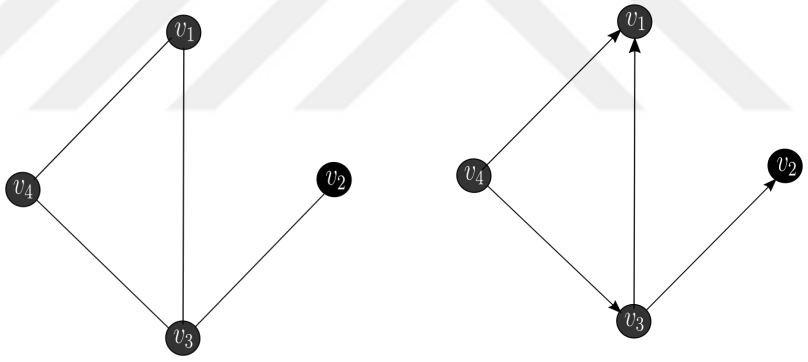

(a) Undirected simple graph (b) Directed simple graph

Figure 4.2: Simple Graphs

Definition 4.1.7. (Bondy and Murty, 1976, p. 4) A **path** is a simple graph whose vertices can be arranged in a linear sequence in such a way that two vertices are adjacent if they are consecutive in the sequence, and are nonadjacent otherwise.

Definition 4.1.8. (Bondy and Murty, 1976, p. 5) An undirected graph is **connected** if, for every partition of its vertex set into two nonempty sets X and Y, there is an edge with one end in X and one end in Y. Otherwise, the graph is disconnected.

Definition 4.1.9. (Agaev and Chebotarev, 2006, pp. 1424–1450; Veerman and Lyons, 2020, pp. 3-4)

(i) A digraph G is **strongly connected** if for every ordered pair of vertices (i, j), there is a path from i to j.

(ii) A digraph G is **unilaterally connected** if for every ordered pair of vertices (i, j), there is a path from i to j or a path from j to i.

(iii) A digraph G is **weakly connected** if the underlying undirected graph is connected.

(iv) A digraph G is **not connected** if it is not weakly connected.

As an alternative to diagrammatic representation of a graph, one might represent a graph in the form of a matrix.

Definition 4.1.10. Given a graph G **the adjacency matrix of** G is $A_G := [a_{ij}] \in M_n$, where

$$a_{ij} = \begin{cases} w & \text{if } (j,i) \in E \\ 0 & \text{otherwise} \end{cases} \tag{4.1}$$

and $w \geq 0, w \in \mathbb{R}$ is the weight of the directed edge starting from vertex j and ending at vertex i which is the convention used in this research.

The element on the ith row and jth column of a matrix A is denoted a_{ij}.

Definition 4.1.11. In a directed graph the **in-degree of a vertex** i denotes the number of edges directed to the vertex i and **out-degree of a vertex** i denotes the number of edges leaving the vertex i. The in-degree of a vertex i is denoted by

$$d_i = \sum_j a_{ij}. \tag{4.2}$$

Definition 4.1.12. (Chebotarev and Agaev, 2013, pp. 1134-1141) A diverging tree is a weakly connected digraph in which one vertex (called the root) has indegree zero and the remaining vertices have indegree one.

Definition 4.1.13. In-degree matrix D_G is a diagonal matrix whose (i, i)-entry is the in-degrees of the vertex i of G.

Definition 4.1.14. L_G is the (combinatorial in-degree) **Laplacian matrix** defined by $L_G := D_G - A_G$ where D_G is the in-degree matrix and A_G is the adjacency matrix of graph G.

By definition, the adjacency and Laplacian matrices of graph G are real.

Definition (4.1.6) implies that adjacency and Laplacian matrices of undirected graph are symmetric, $A = A^T$, i.e., $a_{ij} = a_{ji}$.

When a graph under consideration is dense, representing the graph with matrices is more practical than listing. Aside from the practical use of matrix representations, spectral properties, e.g., the characteristic polynomial, eigenvalues, and eigenvectors of matrices associated with the graph, indicate structural properties, e.g., connectivity and partitioning. In this study, only the Laplacian spectrum is visited due to applicational purposes, even though it is possible to consider other spectra, such as the spectrum of the adjacency matrix.

4.2 Laplacian Spectrum of a Graph

Definition 4.2.1. (Brouwer and Haemers, 2011, p. 3) The **characteristic polynomial** of G is that of L, that is, the polynomial p_L defined by $p_L(\lambda) = det(\lambda I - L)$.

Definition 4.2.2. (Horn and Johnson, 2012, p. 44) Let $L \in M_n$. If a scalar λ and a nonzero vector x satisfy the equation

$$Lx = \lambda x, \quad x \in \mathbb{C}^n, x \neq 0, \lambda \in \mathbb{C} \tag{4.3}$$

then λ is called an **eigenvalue** of L and x is called an **eigenvector** of L associated with λ. The pair λ, x is an **eigenpair** for L.

Definition 4.2.3. (Horn and Johnson, 2012, p. 45) **The Laplacian spectrum** of $L \in M_n$ is the set of all $\lambda \in \mathbb{C}$ that are eigenvalues of L; this set is denoted by $\sigma(L)$.

Definition 4.2.4. The **spectral gap** of L is the the second smallest (with respect to the real-part ordering) eigenvalue λ_2 of all $\lambda \in \mathbb{C}$.

Definition 4.2.5. (Meyer, 2000, p. 510) The **algebraic multiplicity** of is the number of times it is repeated as a root of the characteristic polynomial, i.e.,

$algmult_L(\lambda_i) = a_i$ if and only if $(x - \lambda_1)^{a_1} \cdots (x - \lambda_s)^{a_s} = 0$ is the characteristic equation for L.

Definition 4.2.6. (Meyer, 2000, p. 510) When $algmult_L(\lambda_i) = 1$, λ is called **simple eigenvalue**.

Lemma 4.2.7. Zero is always the eigenvalue of L.

Proof. All the rows of L sum to zero by definition, $L := D - A$. Thus, all ones vector $\mathbf{1}$ is an eigenvector with the corresponding eigenvalue zero,i.e., $L.\mathbf{1} = \mathbf{0} = 0.\mathbf{1}$. □

Theorem 4.2.8. If G has a spanning diverging tree, the zero eigenvalue of the Laplacian matrix L is simple.

Proof. (Agaev and Chebotarev, 2006, pp. 1424–1450) □

Theorem 4.2.9. (Gershgorin, (Horn and Johnson, 2012, p. 387)) Let $A = [a_{ij}] \in M_n$, let

$$R_i(A) = \sum_{i \neq j} |a_{ij}|, \quad i = 1, \ldots n \tag{4.4}$$

denote the deleted absolute row sums of A, and consider the n Gershgorin discs

$$Disc(a_{ii}, R_i) := \{z \in \mathbb{C} : |z - a_{ii}| \leq R_i(A)\}, \quad i = 1, \ldots n \tag{4.5}$$

The eigenvalues of A are in the union of Gershgorin discs

$$G(A) = \bigcup_{i=1}^{n} \{z \in \mathbb{C} : |z - a_{ii}| \leq R_i(A)\} \tag{4.6}$$

Furthermore, if the union of k of the n discs that comprise $G(A)$ forms a set $G_k(A)$ that is disjoint from the remaining $n - k$ discs, then $G_k(A)$ contains exactly k eigenvalues of A, counted according to their algebraic multiplicities.

Proof. (Horn and Johnson, 2012, pp. 388-389) □

Corollary 4.2.10. If λ is an eigenvalue of L,

$$\lambda \in G(L), \quad G(L) = \bigcup_{i=1}^{n} Disc(d_i, d_i) \tag{4.7}$$

which implies $\Re(\lambda) \geq 0$.

Corollary 4.2.11. Using Lemma (4.2.7) and Corollary (4.2.10) which is a result of Gershgorin Disc Theorem, the Laplacian spectrum of $L \in M_n$ given by

$$0 = \lambda_1 \leq \mathrm{Re}(\lambda_2) \ldots \leq \mathrm{Re}(\lambda_n) \tag{4.8}$$

where eigenvalues of L enumerated in increasing order.

Corollary 4.2.12. Since Laplacian matrix $L(G)$ of an undirected graph G is real (Note (4.1)) and symmetric (Note (4.1)), the Laplacian spectrum is real. Furthermore, $L(G)$ is positive semidefinite and singular (see Corollary (4.2.11)). Thus, the Laplacian spectrum $L(G)$ of an undirected graph G is given by

$$0 = \lambda_1 \leq \lambda_2 \ldots \leq \lambda_n \tag{4.9}$$

4.3 Some Special Graphs and Their Laplacian Spectra

Let consider some finite, undirected, and simple graphs and their Laplacian spectra which are the building blocks of our models (Figure 4.3). In this section, we write multiplicities as exponents.

Definition 4.3.1. (Bondy and Murty, 1976, p. 4) A **complete** graph K_n on n vertices is a simple graph in which any two vertices are adjacent.
$\sigma(L_{K_n}) = \{0^1, n^{n-1}\}$
(Brouwer and Haemers, 2011, p. 8).

Definition 4.3.2. (Bondy and Murty, 1976, p. 4) A graph is **bipartite** if its vertex set can be partitioned into two subsets X and Y so that every edge has one end in X and one end in Y. If $G[X, Y]$ is simple, bipartite and every vertex in X is joined to every vertex in Y, then G is called a **complete bipartite graph** $K_{n,m}$.
$\sigma(L_{K_{n,m}}) = \{0^1, m^{n-1}, n^{m-1}, (n+m)^1\}$
(Brouwer and Haemers, 2011, p. 8).

Definition 4.3.3. (Bondy and Murty, 1976, p. 4) A **star** graph S_m is a complete bipartite graph $K_{1,m-1}$ on m vertices.
$\sigma(L_{S_m}) = \{0^1, 1^{m-2}, m^1\}$
(Brouwer and Haemers, 2011, p. 8).

Definition 4.3.4. (Bondy and Murty, 1976, p. 4) A **path** P_n on n vertices is a simple graph whose vertices can be arranged in a linear sequence in such a way that two vertices are adjacent if they are consecutive in the sequence, and are nonadjacent otherwise.

$\sigma(L_{P_n}) = 2 - 2\cos(\pi j/n)$ where $(j = 0, \cdots, n-1)$

(Brouwer and Haemers, 2011, p. 9).

Definition 4.3.5. (Bondy and Murty, 1976, p. 4) A **cycle** C_n on n vertices $(n \geq 3)$ is a simple graph whose vertices can be arranged in a cyclic sequence in such a way that two vertices are adjacent if they are consecutive in the sequence, and are nonadjacent otherwise.

$\sigma(L_{C_n}) = 2 - 2\cos(2\pi j/n)$ where $(j = 0, \cdots, n-1)$

(Brouwer and Haemers, 2011, p. 8).

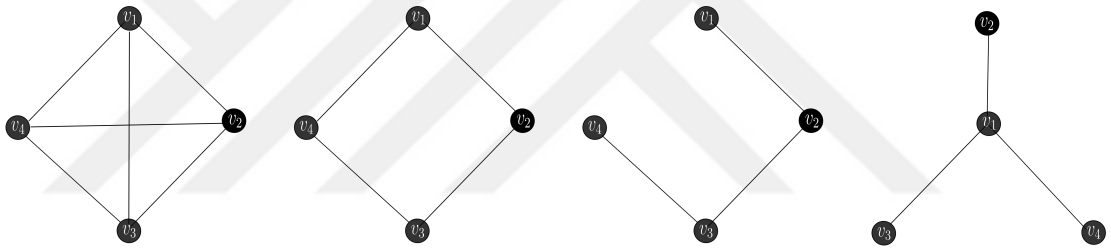

Figure 4.3: K_4, C_4, P_4, S_4, respectively.

5. UNEXPECTED EMERGENT BEHAVIOR IN NETWORK DYNAMICS

5.1 Problem Setting: Cycle-Star Motif

Let G be an arbitrary weighted directed graph whose nodes are labeled by $1, \ldots, n$. We assume that G is unilaterally connected. Then the zero eigenvalue of $L_{\mathcal{G}}$ is simple. The real parts of all the non-zero eigenvalues of L_G are positive by Corollary 4.2.11. Let $\lambda_1, \ldots, \lambda_n$ be the eigenvalues of L_G, ordered according to their real parts, i.e.

$$0 = \lambda_1 \leq \mathrm{Re}(\lambda_2) \ldots \leq \mathrm{Re}(\lambda_n)$$

We discuss how perturbing G can affect its spectral gap. We consider three models, namely model I, model II, and model III, and study them case by case in Theorems A, B and C. Model I is a special case of model II, and model II is a special case of model III. However, the more specific the model is, the stronger results are proved in the mentioned theorems.

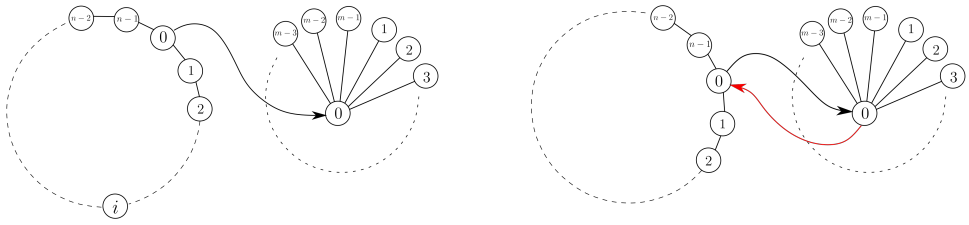

(a) The unperturbed graph G. (b) The perturbed graph G_p.

Figure 5.1: Model I: Breaking the master-slave through hub coupling. We add a directed link from the hub of the star to the cutset node (the red-color edge) where the cutset node refers to the node which cutset edge starts from. The weakly connected directed graph becomes the strongly connected directed graph consequent to the perturbation shown by the red arrow.

Let us start with model I. Let C_n $(n \geq 3)$ and S_m $(m \geq 4)$ be undirected cycle and star graphs, respectively. Label the nodes of C_n and S_m by $0, \ldots, n-1$ and $0, \ldots, m-1$, respectively, such that the hub of the star is labelled by 0. Consider a unilaterally connected digraph G consisting of two strongly connected components

C_n and S_m which are connected together by a directed edge starting from node 0 of the cycle and ending at the hub of the star. Suppose that we perturb this graph by adding a directed link with weight $\delta_0 \geq 0$ starting from the hub of the star and ending at node 0 of the cycle (see Figure 5.1). Denote this perturbed graph by G_p and let $L_{G_p} = L_G(\delta_0)$ be the corresponding Laplacian matrix. Moreover, define

Definition 5.1.1. Consider arbitrary integers $n \geq 3$ and $m \geq 4$, and an arbitrary real number $w \geq 0$. Then

1. for any integer $0 \leq l \leq n$, we define

$$\alpha_l := 2\left(1 - \cos\frac{l\pi}{n}\right). \tag{5.1}$$

2. we define $\beta^-_{m,w}$ and $\beta^+_{m,w}$ as the roots of the quadratic polynomial $\lambda^2 - (m+w)\lambda + w$, i.e.

$$\beta^{\pm}_{m,w} = \frac{1}{2}\left[m + w \pm \sqrt{(m+w)^2 - 4w}\right]. \tag{5.2}$$

Remark 5.1.2. By virtue of Taylor's theorem, we can approximate α_l for sufficiently small $\frac{l}{n}$ by $\alpha_l \approx \frac{l^2\pi^2}{n^2}$. Regarding $\beta^{\pm}_m$, when $(m+w)^2 \gg 4w$, we can approximate β^+_m by $m+w$, and β^-_m by

$$\beta^-_{m,w} = \frac{\beta^-_{m,w}\beta^+_{m,w}}{\beta^+_{m,w}} \approx \frac{w}{m+w}. \tag{5.3}$$

Before we proceed to our first result, let us give some intuition about this definition. The parameter w in $\beta^{\pm}_{m,w}$ stands for the sum of the weights of all the cutset edges starting from the cycle and ending at the star. In the case of model I and II, we assume $w = 1$, but for model III, we deal with arbitrary w. As it is shown later (see Proposition 5.2.3), the spectrum of the unperturbed Laplacian L_G is $\{\alpha_l : \text{where } 0 \leq l \leq n \text{ and } l \text{ is even}\} \cup \{\beta^-_{m,w}, 1, \beta^+_{m,w}\}$. Thus, the spectral gap of L_G is given by $\min\{\alpha_2, \beta^-_{m,w}\}$. Although the α_l's for odd l do not appear as the eigenvalues of L_G, they play an important role in our theory.

Here is our main result on the model I:

Theorem A (Model I). *Assume* $\beta_{m,1}^{-} \notin \{\alpha_l : 0 \leq l \leq n\}$. *Consider an arbitrary perturbation* $\delta_0 > 0$ *and the corresponding Laplacian* $L_{G_p} = L_G(\delta_0)$. *Then, all the eigenvalues of* L_{G_p} *are real. Moreover, we have*

1. *if* $\alpha_1 < \beta_{m,1}^{-}$, *then* $\lambda_2\left(L_{G_p}\right) < \lambda_2\left(L_G\right)$.
2. *if* $\beta_{m,1}^{-} < \alpha_1$, *then* $\lambda_2\left(L_{G_p}\right) > \lambda_2\left(L_G\right)$.

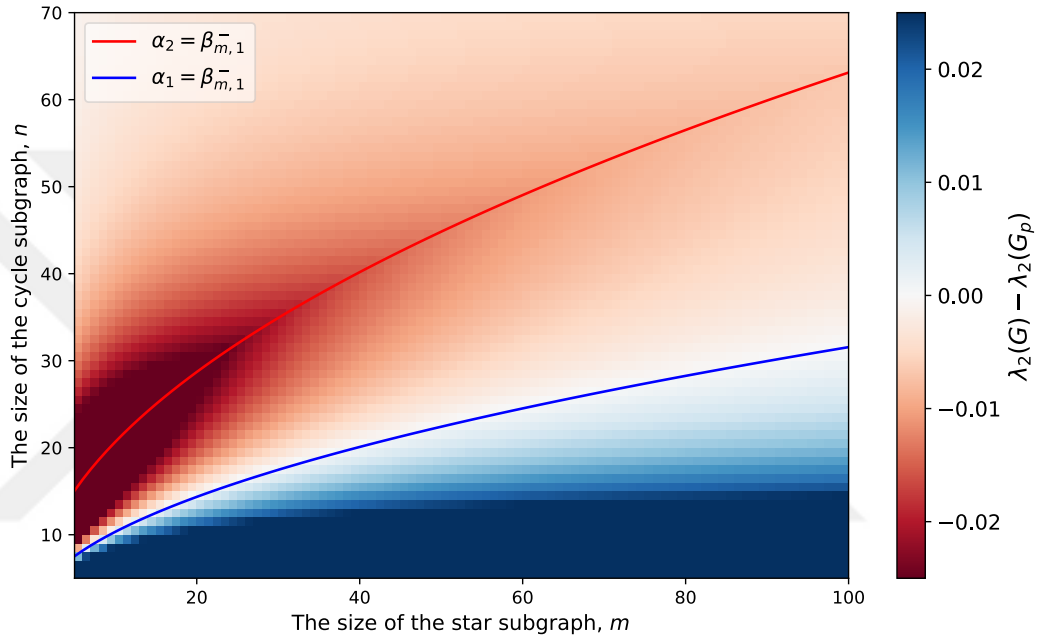

Figure 5.2: A comparison between the Theorem A and the realizations of $\lambda_2(G) - \lambda_2(G_p)$ for chosen sizes of cycle and star subgraphs where $\delta_0 = 1$.

Remark 5.1.3. Note that the assumption $\beta_{m,1}^{-} \notin \{\alpha_l : 0 \leq l < n\}$ in this theorem (and also in the next theorem) is a generic assumption.

In model II, we consider the same unperturbed digraph G as in model I (see Figure (5.3)), but the perturbed graph G_p is generalized. The perturbed graph G_p in model II is given by adding m directed edges starting from each node of the star and ending at node 0 of the cycle. Let $\delta_i \geq 0$ be the weight of the edge starting from node i. Thus, model II is reduced to model I by setting $\delta_i = 0$ for $i = 1, \ldots, m-1$. In this strand, we define

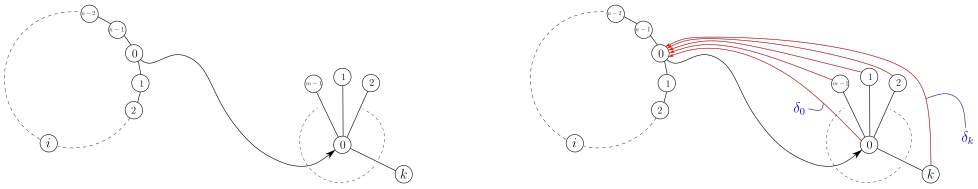

(a) The unperturbed graph G. (b) The perturbed graph G_p.

Figure 5.3: Model II: Breaking the master-slave through multiple couplings. We add links from some nodes of the star to the cutset node of the cycle.

Definition 5.1.4. Let $\delta_i \geq 0$, $i = 0, \ldots, m-1$, be the weight of the perturbation edge starting from node i of the star and ending at node 0 of the cycle. We define $\overline{\delta} := (\delta_0, \ldots, \delta_{m-1})$, and $\delta := \delta_0 + \delta_1 + \cdots + \delta_{m-1}$.

Obviously, $\overline{\delta} = 0$ if and only if $\delta = 0$. Note also that $\delta = 0$ corresponds to the unperturbed graph G. We now state our next main result:

Theorem B. [Model II] Assume $\beta_{m,1}^{-} \notin \{\alpha_l : 0 \leq l < n\}$. Consider a perturbation $\overline{\delta} \neq 0$ and let $L_{G_p} = L_G\left(\overline{\delta}\right)$ be the corresponding Laplacian. Then, the following hold.

1. (Local perturbation) Let $\overline{\delta} \neq 0$ be a sufficiently small perturbation. Then, all the eigenvalues of L_{G_p} are real, and
   (a) If $\alpha_1 < \beta_{m,1}^{-}$, then $\lambda_2\left(L_{G_p}\right) < \lambda_2\left(L_G\right)$.
   (b) If $\beta_{m,1}^{-} < \alpha_1$, then $\lambda_2\left(L_{G_p}\right) > \lambda_2\left(L_G\right)$.
2. (Global perturbation) Let $\overline{\delta} \neq 0$ be an arbitrary perturbation. We have
   (a) If $\alpha_2 < \beta_{m,1}^{-}$, then $\mathrm{Re}\left(\lambda_2\left(L_{G_p}\right)\right) < \lambda_2\left(L_G\right)$.
   (b) Assume the condition $\delta < \delta_0 \beta_{m,1}^{+}$ is satisfied. Then, all the eigenvalues of L_{G_p} are real, and the statements (1a) and (1b) of this theorem also hold for the perturbation $\overline{\delta}$.

Remark 5.1.5. Note that, by setting $\delta = \delta_0$, Theorem A directly follows from Theorem B.

Remark 5.1.6. In spite of Theorem A for which the main statements hold for a perturbation of an arbitrary size, in Theorem B, we require a condition on the perturbation, i.e. $\delta < \delta_0 \beta^+_{m,1}$, to make the statements for perturbations of arbitrary size. Roughly speaking, this is due to the possibility of the emergence of non-real eigenvalues. Indeed, as it is shown in the proof of Theorem B, for small perturbation $\overline{\delta} \neq 0$, the perturbed Laplacian L_{G_p} has two real eigenvalues in the interval (α_{n-1}, ∞). However, as $\overline{\delta}$ varies and gets larger in size, these two real eigenvalues may collide and become a pair of complex conjugates. In this case, we can think of the scenario in which the real part of these eigenvalues decreases such that for some sufficiently large perturbation $\overline{\delta}$, these eigenvalues become the spectral gap of L_{G_p}. By assuming $\delta < \delta_0 \beta^+_{m,1}$, we indeed avoid this scenario.

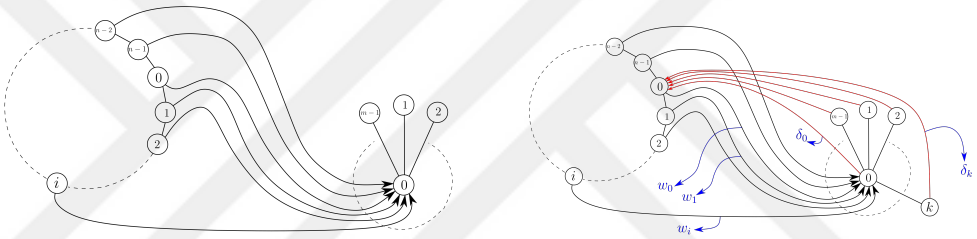

(a) The unperturbed graph G. (b) The perturbed graph G_p.

Figure 5.4: Model III: Breaking the generalized master-slave through multiple couplings. We add links from some nodes of the star to the one cutset node of the cycle where multiple cutset nodes exist.

We now discuss model III. In this model, we consider a more general version of the unperturbed graph of the previous two models. Consider again the graph C_n and S_m as above, and let G be a unilaterally connected digraph consisting of two strongly connected components C_n and S_m which are connected together by n directed edges starting from each node of the cycle and ending at the hub of the star. Let $w_i \geq 0$, where $i = 0, \ldots, n-1$, be the weight of the edge starting from node i of the cycle. Without loss of generality, assume $w_0 > 0$. We also define

Definition 5.1.7. Let w_i be as mentioned above. We define $\overline{w} = (w_0, \ldots, w_{n-1})$ and $w = w_0 + w_1 + \cdots + w_{n-1}$.

It is shown later that $\lambda_2(L_G) = \min\{\alpha_2, \beta^-_{m,w}\}$. Regarding the perturbation in the case of model III, we consider the same family of perturbations as we considered in model II: for every $0 \leq i \leq m-1$, there exists a perturbation edge with weight $\delta_i \geq 0$ starting from node i of the star and ending at node 0 of the cycle (see Figure 5.4). Let $\overline{\delta}$ and δ be as in Definition 5.1.4. For given m, n, $\overline{w}$, δ_0 and δ, in the case that $\alpha_2 \neq \beta^-_{m,w}$, we also define

$$S = S(m, n, \overline{w}, \delta_0, \delta) := \delta - \frac{\delta - \delta_0\alpha_2}{\alpha_2^2 - (m+w)\alpha_2 + w} \sum_{i=0}^{n-1} w_i \cos\frac{2i\pi}{n}. \tag{5.4}$$

As it is shown later, the sign of S determines if the characteristic polynomial of L_{G_p}, i.e. $\det\left(L_{G_p} - \lambda I\right)$, decreases or increases at the point $\lambda = \alpha_2$. Our last result is as follows.

Theorem C. [Model III] Assume $\beta^-_{m,w} \notin \{\alpha_l : 0 \leq l \leq n\}$. Consider a perturbation $\overline{\delta} \neq 0$ and let $L_{G_p} = L_G\left(\overline{\delta}\right)$ be the corresponding Laplacian. Then, the following hold.

1. (Local perturbation) Let $\overline{\delta} \neq 0$ be sufficiently small. Then, all the eigenvalues of L_{G_p} are real, and we have
   (a) If $\alpha_2 < \beta^-_{m,w}$ and $S < 0$, then $\lambda_2\left(L_{G_p}\right) < \lambda_2(L_G)$.
   (b) If $\alpha_2 < \beta^-_{m,w}$ and $S > 0$, then $\lambda_2\left(L_{G_p}\right) = \lambda_2(L_G)$.
   (c) If $0 < \beta^-_{m,w} < \alpha_1$, then $\lambda_2\left(L_{G_p}\right) > \lambda_2(L_G)$.
   (d) If $\alpha_1 < \beta^-_{m,w} < \alpha_2$ and $\sum_{i=0}^{n-1} w_i \cos\left(\frac{n}{2} - i\right)\theta > 0$, where $\theta = \pi - \cos^{-1}\left(\frac{\beta^-_{m,w}-2}{2}\right)$, then $\lambda_2\left(L_{G_p}\right) > \lambda_2(L_G)$.
   (e) If $\alpha_1 < \beta^-_{m,w} < \alpha_2$ and $\sum_{i=0}^{n-1} w_i \cos\left(\frac{n}{2} - i\right)\theta < 0$, where $\theta = \pi - \cos^{-1}\left(\frac{\beta^-_{m,w}-2}{2}\right)$, then $\lambda_2\left(L_{G_p}\right) < \lambda_2(L_G)$.
2. (Global perturbation) Let $\overline{\delta} \neq 0$ be an arbitrary perturbation and assume $\alpha_2 < \beta^-_{m,w}$.
   (a) If $S < 0$, then $\mathrm{Re}\left(\lambda_2\left(L_{G_p}\right)\right) < \lambda_2(L_G)$.
   (b) If $S > 0$, then $\mathrm{Re}\left(\lambda_2\left(L_{G_p}\right)\right) \leq \lambda_2(L_G)$.

5.2 The Laplacian L_G of the Unperturbed Graph and Its Spectrum

Denote the Laplacian matrices of the cycle C_n and the star S_m by L_{C_n} and L_{S_m}, respectively. Then

$$L_G := \begin{pmatrix} L_{C_n} & 0 \\ -C & L_{S_m} + D_C \end{pmatrix}, \tag{5.5}$$

where

$$L_{C_n} = \begin{pmatrix} 2 & -1 & 0 & \cdots & 0 & -1 \\ -1 & 2 & -1 & \ddots & & 0 \\ 0 & -1 & \ddots & \ddots & \ddots & \vdots \\ \vdots & \ddots & \ddots & \ddots & \ddots & 0 \\ 0 & & \ddots & \ddots & \ddots & -1 \\ -1 & 0 & \cdots & 0 & -1 & 2 \end{pmatrix}, \; L_{S_m} = \begin{pmatrix} m-1 & -\mathbf{1}_{m-1}^{\top} \\ -\mathbf{1}_{m-1} & I_{(m-1)\times(m-1)} \end{pmatrix}. \tag{5.6}$$

Moreover, for models I and II, we have

$$C = \begin{pmatrix} 1 & 0_{1\times(n-1)} \\ 0_{(m-1)\times 1} & 0_{(m-1)\times(n-1)} \end{pmatrix}, \; D_C = \begin{pmatrix} 1 & 0_{1\times(m-1)} \\ 0_{(m-1)\times 1} & 0_{(m-1)\times(m-1)} \end{pmatrix}, \tag{5.7}$$

and for model III, we have

$$C = \begin{pmatrix} w_0 & w_1 & \cdots & w_{n-1} \\ & 0_{(m-1)\times n} & & \end{pmatrix}, \; D_C = \begin{pmatrix} w & 0_{1\times(m-1)} \\ 0_{(m-1)\times 1} & 0_{(m-1)\times(m-1)} \end{pmatrix}. \tag{5.8}$$

The triangular form of L_G implies $\sigma(L_G) = \sigma(L_{C_n}) \cup \sigma(L_{S_m} + D_C)$. Thus, to study $\sigma(L_G)$, we need to investigate each of $\sigma(L_{C_n})$ and $\sigma(L_{S_m} + D_C)$ individually. In this strand, we have the following lemmas.

Lemma 5.2.1. $\sigma(L_{C_n}) = \{\alpha_l : \text{where } 0 \leq l \leq n \text{ and } l \text{ is even}\}$. Moreover, the multiplicity of all the eigenvalues except for 0 and 4 (the eigenvalue 4 appears only when n is even) is 2.

Proof. (Brouwer and Haemers, 2011, p. 8). □

Lemma 5.2.2. Let C and D_C be as in (5.8). Then, $\sigma(L_{S_m} + D_C) = \{\beta_{m,w}^-, 1, \beta_{m,w}^+\}$, where $\beta_{m,w}^{\pm}$ are as in (5.2). Moreover, the eigenvalues $\beta_{m,w}^-$ and $\beta_{m,w}^+$ are simple, and the eigenvalue 1 is of multiplicity $m-2$.

Proof. This lemma is a special case of Lemma A.0.2 which is proved in Appendix. □

The previous two lemmas determine the spectrum of the unperturbed Laplacian L_G.

Proposition 5.2.3. We have $\sigma(L_G) = \{\alpha_l : \text{where } 0 \leq l \leq n \text{ and } l \text{ is even}\} \cup \{\beta^-_{m,w}, 1, \beta^+_{m,w}\}$.

Remark 5.2.4. In this research, we assumed that $m \geq 4$, i.e. the star S_m has at least four nodes. It is straightforward to show that for any $m \geq 4$ and $w > 0$, we have $\beta^-_{m,w} < 1$ and $4 < \beta^+_{m,w}$. On the other hand, $0 \leq \alpha_l = 2\left(1 - \cos\frac{l\pi}{n}\right) \leq 4$, for all $0 \leq l \leq n$. This means that $\beta^+_{m,w}$ is a simple eigenvalue of L_G.

5.3 The Laplacian L_{G_p} of the Perturbed Graph

Consider model III and observe that the perturbed Laplacian matrix L_{G_p} is given by

$$L_{G_p} := \begin{pmatrix} L_{C_n} + D_\Delta & -\Delta \\ -C & L_{S_m} + D_C \end{pmatrix}, \tag{5.9}$$

where C and D_C are as in (5.8),

$$\Delta = \begin{pmatrix} \delta_0 & \delta_1 & \cdots & \delta_{m-1} \\ & 0_{(n-1)\times m} & & \end{pmatrix} \quad \text{and} \quad D_\Delta = \begin{pmatrix} \delta & 0_{1\times(n-1)} \\ 0_{(n-1)\times 1} & 0_{(n-1)\times(n-1)} \end{pmatrix}. \tag{5.10}$$

Notation 5.3.1. For the sake of convenience, we set $L_1 := L_{C_n} + D_\Delta$ and $L_2 := L_{S_m} + D_C$.

Using this notation, Laplacian (5.9) is written as

$$L_{G_p} = \begin{pmatrix} L_1 & -\Delta \\ -C & L_2 \end{pmatrix}. \tag{5.11}$$

The Laplacian L_{G_p} of the perturbed graph of model II is of the form (5.11), where C and D_C are as in (5.7), and Δ and D_Δ are given by (5.10).

The Laplacian L_{G_p} of the perturbed graph of model I is also of the form (5.11), where C and D_C are as in (5.7), and Δ and D_Δ are given by

$$\Delta = \begin{pmatrix} \delta_0 & 0_{1\times(m-1)} \\ 0_{(n-1)\times 1} & 0_{(n-1)\times(m-1)} \end{pmatrix} \quad \text{and} \quad D_\Delta = \begin{pmatrix} \delta & 0_{1\times(n-1)} \\ 0_{(n-1)\times 1} & 0_{(n-1)\times(n-1)} \end{pmatrix}. \tag{5.12}$$

Here (model I), we have $\delta_0 = \delta$.

Notice that, in all these three models, despite the unperturbed Laplacian L_G, the perturbed Laplacian L_{G_p} does not have a triangular form. Due to this reason, analysis of the spectrum of L_{G_p} requires further work.

5.4 Synchronization in Networks with Cycle-Star Topology

We consider the following settings for the model given in Figure (5.3): Two networks $\mathcal{G} = (G, f, H)$ and $\mathcal{G}_p = (G_p, f, H)$ generated where G and G_p are the unperturbed and the perturbed graphs, respectively. The chosen isolated dynamics f is the Lorenz oscillator given by equation (2.10) where the parameters are $\sigma = 10$, $\gamma = 28$, $\beta = 8/3$. Here, H is the identity function on $\mathbb{R}^3$. For the described setting, equation (3.14) can be written as $\Theta_c = \frac{\kappa}{\mathrm{Re}(\lambda_2)}$, where κ is the largest Lyapunov exponent of the corresponding attractor (Eroglu, Lamb and Pereira, 2017, pp. 207-243). We numerically find that $\kappa \approx 0.9$. So, the expected values of $\Theta_c(\mathcal{G})$ and $\Theta_c(\mathcal{G}_p)$ are calculated accordingly. We examine two experiments to reveal how link addition(s) can lead to synchronization in the network $\mathcal{G}_p$ or break the synchronization in the initial network $\mathcal{G}$ (see Figure 5.5 and 5.6). Networks of coupled chaotic oscillators in model II are simulated to show the synchronization error at a given time, which can be given approximately as

$$E = \sum_{i,j=1}^{n+m} \frac{\|x_i(t) - x_j(t)\|}{(n+m)^2} \tag{5.13}$$

where n, m are the number of nodes of the cycle and the star subgraphs, respectively.

5.4.1 Hindering synchronization

In order to examine the hindrance of synchronization due to link addition(s), the overall coupling constant Θ is selected such that $\Theta_c(\mathcal{G}) < \Theta < \Theta_c(\mathcal{G}_p)$ (see Figure 5.5). Note that such Θ values only exist when $\lambda_2(G) > \lambda_2(G_p)$ due to the order

relations of synchronizability stated above. When the selected Θ is above the $\Theta_c(\mathcal{G})$, the trajectories synchronize for the network $\mathcal{G}$. Then, the system is perturbed by adding link(s) at a given time t. Since the selected Θ is below the $\Theta_c(\mathcal{G}_p)$, the system losses its synchronization thereafter.

In model II, the sizes of the cycle and star subgraphs are set to $n = 15$ and $m = 15$. The weights of the cutset and perturbation edges are $w_0 = 1$ and $\delta_i = 1$, where $i = 0, 1, \cdots, m-1$. Each component of all initial states is randomly selected from the uniform distribution over the $[3.5, 5)$.

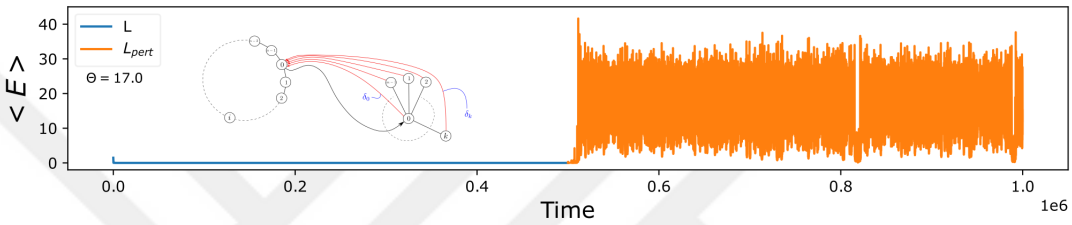

Figure 5.5: Hindrance of Synchronization due to link additions: Networks of coupled chaotic oscillators in model II are simulated to show the synchronization error at a given time, which is given as $E = \sum_{i,j=1} \frac{\|x_i(t)-x_j(t)\|}{(n+m)^2}$ where n, m are the number of nodes of the cycle and the star subgraphs, respectively. After the red links are added to the system at time=0.5×10^6, the synchronization loss occurs where the overall coupling constant Θ is selected as $\Theta_c(\mathcal{G}) < \Theta < \Theta_c(\mathcal{G}_p)$.

5.4.2 Enhancing synchronization

In order to examine the enhance of synchronization due to link addition(s), the overall coupling constant Θ is selected such that $\Theta_c(\mathcal{G}_p) < \Theta < \Theta_c(\mathcal{G})$ (see Figure 5.6). Note that such Θ values only exist when $\lambda_2(G_p) > \lambda_2(G)$. When the selected Θ is below the $\Theta_c(\mathcal{G})$, the trajectories cannot synchronize for the network $\mathcal{G}$. Then, the system is perturbed by adding link(s) at a given time t. Since the selected Θ is above the $\Theta_c(\mathcal{G}_p)$, the system gets into synchronization thereafter.

In model II, the sizes of the cycle and star subgraphs are set to $n = 9$ and $m = 15$. The weights of the cutset and perturbation edges are $w_0 = 1$ and $\delta_i = 1$, where $i = 0, 1, \cdots, m-1$. Each component of all initial states is randomly selected from the uniform distribution over the $[3.5, 5)$.

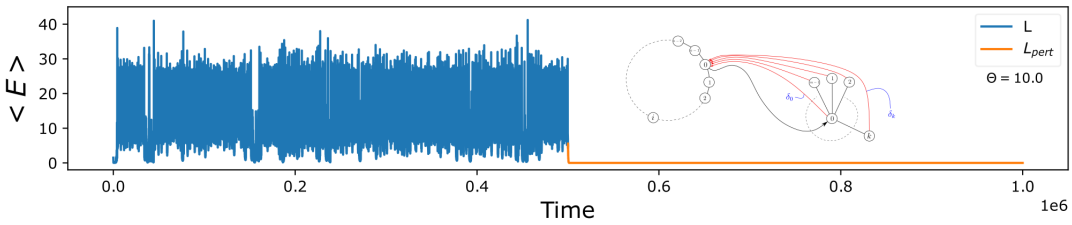

Figure 5.6: Enhance of Synchronization due to link additions: Networks of coupled chaotic oscillators in model II are simulated to show the synchronization error at a given time, which is given as $E = \sum_{i,j=1} \frac{\|x_i(t)-x_j(t)\|}{(n+m)^2}$ where n, m are the number of nodes of the cycle and the star subgraphs, respectively. After the red links are added to each system at time=0.5×10^6, the synchronization occurs where the overall coupling constant Θ is selected as $\Theta_c(\mathcal{G}_p) < \Theta < \Theta_c(\mathcal{G})$.

Therefore, hindrance and enhancement of synchronization due to link additions manifest themselves in simulations as predicted by our theorems.

6. PROOFS OF THE MAIN RESULTS

6.1 Proofs of the Main Results

In this section, we prove Theorem B and Theorem C. Note that, Theorem A follows from Theorem B (See Remark 5.1.5). Furthermore, model II can be considered as a special case of model III. Thus, we first introduce the main concepts and notations that we use in the proofs mainly based on model III.

Definition 6.1.1. Let w, δ_0 and δ be real, and m and k be positive integers. Consider $\lambda \in \mathbb{R}$.

1. We define $\mu : \lambda \mapsto \mu(\lambda)$ by

$$\mu = \mu(\lambda) = \frac{1-\lambda}{\lambda^2 - (m+w)\,\lambda + w}, \tag{6.1}$$

and $y : \lambda \mapsto y(\lambda)$ by

$$y = y(\lambda) = \frac{\delta - \delta_0 \lambda}{\lambda^2 - (m+w)\,\lambda + w}. \tag{6.2}$$

2. For any $k \geq 3$, we define

$$Q_k = Q_k(\lambda) = \begin{pmatrix} \lambda-2 & 1 & & & \\ 1 & \lambda-2 & 1 & & 0 \\ & 1 & \ddots & \ddots & \\ 0 & & \ddots & \ddots & 1 \\ & & & 1 & \lambda-2 \end{pmatrix}_{k\times k}. \tag{6.3}$$

The next two lemmas investigate the matrix $Q_k(\lambda)$ for different values of $\lambda > 0$. See (Hu and O'Connell, 1996, pp. 1511-1513) for the proofs[2] .

Lemma 6.1.2. Assume $0 < \lambda < 4$ and let $\theta = \pi - \cos^{-1}(\frac{\lambda-2}{2})$. We have

1. $\det(Q_k) = \frac{(-1)^k \sin(k+1)\theta}{\sin\theta}$.

[2]Regarding Lemma 6.1.2, the formulas in (Hu and O'Connell, 1996, pp. 1511-1513) are not totally correct. In this research, we have used the corrected ones. Note also that θ in this research is not the same as in (Hu and O'Connell, 1996, pp. 1511-1513)

2. the matrix $R = Q_k^{-1}$ exists for $\theta \neq \frac{l\pi}{k+1}$ $(l = 1, \ldots, k)$, and is given by

$$R_{ij} = \frac{\cos\left(k+1-|i-j|\right)\theta - \cos\left(k+1-i-j\right)\theta}{2\sin\theta\sin\left(k+1\right)\theta}, \qquad \text{for } 1 \leq i, j \leq k. \tag{6.4}$$

Lemma 6.1.3. Assume $\lambda \geq 4$ and let $\theta = \cosh^{-1}(\frac{\lambda-2}{2})$. Then

1. for $\lambda > 4$, we have $\det(Q_k) = \frac{\sinh(k+1)\theta}{\sinh\theta}$.
2. for $\lambda = 4$, we have $\det(Q_k) = k + 1$.
3. The inverse matrix $R = Q_k^{-1}$ exists for all $\lambda \geq 4$, and is given by

$$R_{ij} = (-1)^{i+j} \cdot \frac{\cosh\left(k+1-|i-j|\right)\theta - \cosh\left(k+1-i-j\right)\theta}{2\sinh\theta\sinh\left(k+1\right)\theta}, \qquad \text{for } 1 \leq i, j \leq k. \tag{6.5}$$

Recall α_l is defined by (5.1). By Lemmas 6.1.2 and 6.1.3, and a straightforward calculation, we have

Lemma 6.1.4. The matrix $Q_{n-1}(\lambda)$ is invertible if and only if $\lambda \neq \alpha_l$ for $l = 1, \ldots, n-1$.

6.2 Our Approach for Investigating the Spectrum of the Perturbed Laplacian L_{G_p}

In this section, we discuss the method that we use to investigate the spectrum of the perturbed Laplacian L_{G_p}. We directly apply this method to study model III and then use the results to investigate the models I and II.

Recall that the perturbed Laplacian of model III is given by

$$L_{G_p} = \begin{pmatrix} L_1 & -\Delta \\ -C & L_2 \end{pmatrix}, \tag{6.6}$$

where L_1 and L_2 are as in Notation 5.3.1, and the matrices C and Δ are given by (5.8) and (5.10), respectively. Our study of the eigenvalues of L_{G_p} is based on the following lemma.

Lemma 6.2.1. Consider the perturbed Laplacian L_{G_p} given by (6.6). For $\lambda \in \mathbb{R}$, we have

1. if $\lambda \notin \sigma(L_1)$, then $\det\left(L_{G_p} - \lambda I\right) = \det\left(L_1 - \lambda I\right) \cdot P_1\left(\lambda\right)$, where $P_1(\lambda) = \det(M_1)$, for $M_1 = M_1(\lambda) = L_2 - \lambda I - C\left(L_1 - \lambda I\right)^{-1}\Delta$.

2. if $\lambda \notin \sigma(L_2)$, then $\det\left(L_{G_p} - \lambda I\right) = \det\left(L_2 - \lambda I\right) \cdot P_2\left(\lambda\right)$, where $P_2(\lambda) = \det(M_2)$, for $M_2 = M_2(\lambda) = L_1 - \lambda I - \Delta\left(L_2 - \lambda I\right)^{-1} C$.

3. for $i = 1, 2$, we have that $\lambda_0 \notin \sigma(L_i)$ is an eigenvalue of L_{G_p} with algebraic multiplicity k, if and only if $P_i(\lambda_0) = P_i'(\lambda_0) = \cdots = \frac{d^{k-1}P_i}{d\lambda^{k-1}}(\lambda_0) = 0$, and $\frac{d^k P_i}{d\lambda^k}(\lambda_0) \neq 0$.

Remark 6.2.2. Lemma 6.2.1 allows us to count the multiplicity of $\lambda_0 \in \sigma(L_{G_p})$ when $\lambda_0 \notin \sigma(L_1) \cap \sigma(L_2)$. However, this lemma may give information about the multiplicity of λ_0 when $\lambda_0 \in \sigma(L_1) \cap \sigma(L_2)$ as well. This is important for us since we have such eigenvalues in our models. Let λ_0 be such an eigenvalue. Since $\lambda_0 \in \sigma(L_1)$, the matrix $(L_1 - \lambda_0 I)^{-1}$ does not exist. However, depending on the matrices C and Δ, the expression $\lim_{\lambda \to \lambda_0} Y(\lambda)$, where $Y(\lambda) := C(L_1 - \lambda_0 I)^{-1}\Delta$, may exist. This allows us to define M_1 and P_1 at $\lambda = \lambda_0$ by taking the limit $\lambda \to \lambda_0$. Now, if $Y(\lambda)$ at $\lambda = \lambda_0$ is smooth enough, then the multiplicity of λ_0 as an eigenvalue of L_{G_p} is $l + k$, where l is the multiplicity of λ_0 as an eigenvalue of L_1 and k is the integer that satisfies $P_1(\lambda_0) = P_1'(\lambda_0) = \cdots = \frac{d^{k-1}P_1}{d\lambda^{k-1}}(\lambda_0) = 0$, and $\frac{d^k P_1}{d\lambda^k}(\lambda_0) \neq 0$. Analogous holds when $\lambda_0 \in \sigma(L_2)$ but $\Delta\left(L_2 - \lambda I\right)^{-1} C$ is well-defined and smooth enough at $\lambda = \lambda_0$.

According to Lemma 6.2.1, an eigenvalue λ of L_{G_p} that is not in $\sigma(L_1) \cap \sigma(L_2)$ must satisfy $P_1(\lambda) = 0$ or $P_2(\lambda) = 0$. The proofs of our results are based on the analysis of these two equations. Sections 6.2 and 6.2.1 are dedicated to this analysis.

Before we proceed further, let us show that $\lambda = 1$ is an eigenvalue of L_{G_p} for any arbitrary $\overline{\delta}$.

Lemma 6.2.3. For arbitrary $\overline{\delta}$, we have $1 \in \sigma(L_{G_p})$. Moreover, the (algebraic and geometric) multiplicity of 1 is at least $m - 2$.

Proof. Recall that $L_{G_p} = \begin{pmatrix} L_1 & -\Delta \\ -C & L_2 \end{pmatrix}$. It follows from the proof of Lemma A.0.2 (see relation (A.4)) that there exist $m-2$ linearly independent left eigenvectors v such

that $v^\top L_2 = v^\top$. Moreover, any such a vector v is of the form $v = (0, v_1, \cdots, v_{m-1}) \in \mathbb{R}^m$ (the first entry is zero). Consider the vector $u := (0, v) \in \mathbb{R}^{n+m}$. Taking into account that, except for the first row, all the entries of C are zero (see (5.8)), we obtain

$$u^\top L_{G_p} = \left(0_{1\times n}, v^\top\right) \begin{pmatrix} L_1 & -\Delta \\ -C & L_2 \end{pmatrix} = \left(0_{1\times n}, v^\top L_2\right) = u^\top.$$

This means that for such vs, the corresponding vectors u are left eigenvectors of L_{G_p} associated with the eigenvalue 1. This proves the lemma. □

Analysis of P_2. In this section, we investigate the matrix $M_2(\lambda)$ and the function $P_2(\lambda) := \det(M_2(\lambda))$ introduced in Lemma 6.2.1 for model III. We first need to analyze the matrix $L_2 - \lambda I$ and its inverse:

Lemma 6.2.4. *Recall μ from (6.1). We have*

1. *the function μ is well-defined at $\lambda \notin \{\beta^-_{m,w}, \beta^+_{m,w}\}$.*
2. *for $\lambda \in \mathbb{R} \setminus \sigma(L_2) = \{\beta^-_{m,w}, 1, \beta^+_{m,w}\}$, we have*

$$(L_2 - \lambda I)^{-1} = \begin{pmatrix} m-1+w-\lambda & -\mathbf{1}^\top \\ -\mathbf{1} & (1-\lambda)\, I \end{pmatrix}^{-1} = \begin{pmatrix} \mu & \frac{\mu}{1-\lambda}\mathbf{1}^\top \\ \frac{\mu}{1-\lambda}\mathbf{1} & \frac{1}{1-\lambda} I + \frac{\mu}{(1-\lambda)^2}\mathbf{1}\mathbf{1}^\top \end{pmatrix}. \tag{6.7}$$

Proof. The first part of the statement is straightforward. The second part follows from Lemma A.0.1. □

We now start to calculate $M_2 = M_2(\lambda) = L_1 - \lambda I - \Delta\,(L_2 - \lambda I)^{-1}\, C$. The expression $(L_2 - \lambda I)^{-1}$ is well-defined at $\lambda \notin \sigma(L_2) = \{\beta^-_{m,w}, 1, \beta^+_{m,w}\}$. By a straightforward calculation and using relation (6.7), for $\lambda \notin \sigma(L_2)$, we have $\Delta\,(L_2 - \lambda I)^{-1}\, C = yC$, where $y = y(\lambda)$ is given by (6.2). Note that y, and therefore yC, is well-defined and smooth at $\lambda = 1$. In other words, although $(L_2 - \lambda I)^{-1}$ is not defined at $\lambda = 1$ (because $1 \in \sigma(L_2)$), the expression $\Delta\,(L_2 - \lambda I)^{-1}\, C$ can be defined at $\lambda = 1$, and so do the matrix M_2 and the function P_2. This was discussed earlier in Remark 6.2.2. We give the following lemma to emphasize on this property.

Lemma 6.2.5. The function $P_2(\lambda) = \det(M_2)$ is well-defined and smooth at $\lambda \notin \{\beta^-_{m,w}, \beta^+_{m,w}\}$.

Having $\Delta (L_2 - \lambda I)^{-1} C = yC$, we obtain

$$M_2 = M_2(\lambda) = \left(\begin{array}{c|ccccc} 2-\lambda+\delta-w_0 y & -1-w_1 y & -w_2 y & \cdots & w_{n-2} y & -1-w_{n-1} y \\ \hline -1 & & & & & \\ 0_{(n-3)\times 1} & & & -Q_{n-1} & & \\ -1 & & & & & \end{array}\right), \tag{6.8}$$

where $Q_{n-1} = Q_{n-1}(\lambda)$ is the symmetric tridiagonal matrix given by (6.3). Applying Lemma A.0.1 on this matrix, for $\lambda \notin \{\beta^-_{m,w}, \beta^+_{m,w}\}$ such that $Q_{n-1}(\lambda)$ is invertible (recall that, by Lemma 6.1.4, the matrix $Q_{n-1}(\lambda)$ is invertible if and only if $\lambda \neq \alpha_l$ for $l = 1, \ldots, n-1$), we obtain

$$P_2(\lambda) = \det(M_2) = (-1)^{n-1} \det(Q_{n-1}) \left[\xi(\delta, \lambda) - y\psi(w, \lambda)\right], \tag{6.9}$$

where

$$\xi(\delta, \lambda) = 2 - \lambda + \delta + R_{11} + R_{1\,n-1} + R_{n-1\,1} + R_{n-1\,n-1}, \tag{6.10}$$

for which $R = (R_{ij})_{1 \leq i,j \leq n-1}$ is the inverse of Q_{n-1}, and

$$\psi = \psi(\overline{w}, \lambda) = w_0 - \sum_{i=1}^{n-1} w_i \left[R_{i1} + R_{i\,n-1}\right]. \tag{6.11}$$

Lemmas 6.1.2 and 6.1.3 give some formulas for $R = Q_{n-1}^{-1}$. Substituting these formulas in (6.10) and (6.11) gives

Lemma 6.2.6. For the functions $\xi(\delta, \lambda)$ and $\psi(\overline{w}, \lambda)$, we have

$$\xi = \xi(\delta, \lambda) = \begin{cases} \delta - 2\sin\theta \tan\frac{n\theta}{2}, & 0 < \lambda < 4 \text{ and } \theta = \pi - \cos^{-1}(\frac{\lambda-2}{2}), \\ \delta + \frac{2}{n} \cdot \left[(-1)^n - 1\right], & \lambda = 4, \\ \delta + \frac{2\sinh\theta}{\sinh n\theta} \cdot \left[(-1)^n - \cosh n\theta\right], & \lambda > 4 \text{ and } \theta = \cosh^{-1}(\frac{\lambda-2}{2}), \end{cases}$$

and

$$\psi = \psi(\overline{w}, \lambda) = \begin{cases} \frac{1}{\cos\frac{n\theta}{2}} \sum_{i=0}^{n-1} w_i \cos\left(\frac{n}{2} - i\right)\theta, & 0 < \lambda < 4 \text{ and } \theta = \pi - \cos^{-1}(\frac{\lambda-2}{2}), \\ \sum_{i=0}^{n-1} (-1)^i w_i, & n \text{ is even, } \lambda = 4, \\ \sum_{i=0}^{n-1} (-1)^i w_i \left[1 - \frac{2i}{n}\right], & n \text{ is odd, } \lambda = 4, \\ \frac{1}{\cosh\frac{n\theta}{2}} \sum_{i=0}^{n-1} (-1)^i w_i \cosh\left(\frac{n}{2} - i\right)\theta, & n \text{ is even, } \lambda > 4 \text{ and } \theta = \cosh^{-1}(\frac{\lambda-2}{2}), \\ \frac{1}{\sinh\frac{n\theta}{2}} \sum_{i=0}^{n-1} (-1)^i w_i \sinh\left(\frac{n}{2} - i\right)\theta, & n \text{ is odd, } \lambda > 4 \text{ and } \theta = \cosh^{-1}(\frac{\lambda-2}{2}). \end{cases}$$

Proof. For $\lambda \neq 4$, the proof is a straightforward calculation by substituting (6.4) and (6.5) into (6.10) and (6.11). For the case of $\lambda = 4$, the proof follows from taking the limit of the formulas for the cases $\lambda \neq 4$ as $\lambda \to 4$ and using L'Hôpital's rule. □

This lemma together with relation (6.9), gives some formulas for $P_2(\lambda)$ when P_2 is well-defined ($\lambda \notin \{\beta^-_{m,w}, \beta^+_{m,w}\}$) and $Q_{n-1}(\lambda)$ is invertible, i.e. $\lambda \neq \alpha_l$ for $l = 1, \ldots, n-1$. However, we can use (6.9) to calculate P_2 at $\lambda = \alpha_l$ by taking $\lim P_2(\lambda)$ as $\lambda \to \alpha_l$. By this trick, we have that (6.9) is well-defined and smooth at every real $\lambda \notin \{\beta^-_{m,w}, \beta^+_{m,w}\}$.

To make the analysis of P_2 simpler, we consider two different cases of $0 \leq \lambda < 4$ and $\lambda \geq 4$. For the first case, let $\theta = \pi - \cos^{-1}(\frac{\lambda-2}{2})$, and define $p(\theta) := P_2(\lambda(\theta)) = P_2(2[1-\cos\theta])$. For $0 < \theta < \pi$ such that $2[1-\cos\theta] \notin \{\beta^-_{m,w}, \beta^+_{m,w}\}$, this gives

$$p(\theta) = 2[\cos n\theta - 1] + \delta \cdot \frac{\sin n\theta}{\sin\theta} - 2y \cdot \frac{\sin\frac{n\theta}{2}}{\sin\theta} \sum_{i=0}^{n-1} w_i \cos\left(\frac{n}{2} - i\right)\theta. \tag{6.12}$$

Observe that $p(0) = \lim_{\theta\to 0^+} p(\theta) = 0$. With a straightforward calculation, we can also obtain:

Lemma 6.2.7. Recall α_l given by (5.1) and assume $\alpha_l = 2\left(1-\cos\frac{l\pi}{n}\right) \notin \{\beta^-_{m,w}, \beta^+_{m,w}\}$, where $l \in \mathbb{Z}$ is as specified below. Then

1. for even $0 \leq l \leq n-1$, we have $p(\frac{l\pi}{n}) = 0$.
2. for odd $1 \leq l \leq n-1$, we have $p(\frac{l\pi}{n}) = -4 - \frac{2y}{\sin\frac{l\pi}{n}} \sum_{i=0}^{n-1} w_i \sin\frac{il\pi}{n}$.
3. for even $1 \leq l \leq n-1$, we have

$$p'\left(\frac{l\pi}{n}\right) = \frac{n}{\sin\frac{l\pi}{n}}\left[\delta - y\sum_{i=0}^{n-1} w_i \cos\frac{il\pi}{n}\right]. \tag{6.13}$$

6.2.1 Analysis of P_1

In this section, we investigate the matrix M_1 and the function $P_1(\lambda) = \det(M_1(\lambda))$ introduced in Lemma 6.2.1 for model III. We start with analyzing the matrix $L_1 - \lambda I$

and its inverse. Note that

$$L_1 - \lambda I = \left(\begin{array}{c|cc} 2+\delta-\lambda & -1 & 0_{1\times(n-3)} \quad -1 \\ \hline -1 & & \\ 0_{(n-3)\times 1} & & -Q_{n-1} \\ -1 & & \end{array}\right). \tag{6.14}$$

Lemma 6.2.8. Let $\lambda > 0$ be real. Then, the matrix $L_1 - \lambda I$ is invertible if and only if $\lambda \neq \alpha_l$ and $\xi(\delta, \lambda) \neq 0$, where $1 < l \leq n-1$ is even and $\xi(\delta, \lambda)$ is given by (6.10).

Proof. Assume Q_{n-1} is invertible. Applying Lemma A.0.1 on matrix (6.14) gives

$$\det(L_1 - \lambda I) = (-1)^{n-1} \det(Q_{n-1})\, \xi(\delta, \lambda).$$

This proves the lemma for the case that Q_{n-1} is invertible.

Now, we consider the case that Q_{n-1} is singular. It follows from Lemma 6.1.4 that$Q_{n-1}(\lambda)$ is invertible if and only if $\lambda \neq \alpha_l$ for $l = 1, \ldots, n-1$. Equivalently Q_{n-1} is singular if and only if $0 < \lambda = 2[1 - \cos\theta_0] < 4$ and $\sin n\theta_0 = 0$ (see also Lemmas 6.1.2 and 6.1.3). By virtue of Lemma 6.2.6, for $\lambda = 2[1 - \cos\theta_0]$, we obtain

$$\det(L_1 - \lambda I) = \lim_{\theta\to\theta_0} \det(L_1 - \lambda I) = \lim_{\theta\to\theta_0} \frac{\sin n\theta}{\sin\theta} \cdot \left(\delta - 2\sin\theta \tan\frac{n\theta}{2}\right) = 2(\cos n\theta_0 - 1).$$

Thus, when Q_{n-1} is singular, $L_1 - \lambda I$ is invertible if and only if $\cos n\theta_0 \neq 1$, i.e. $\lambda \neq \alpha_l$ where $2 \leq l \leq n-1$ is even. This ends the proof. □

For real $\lambda > 0$, assume $\xi(\delta, \lambda) \neq 0$ and consider the case that $R = Q_{n-1}^{-1}$ exists. Then, $L_1 - \lambda I$ is invertible, and by Lemma A.0.1, we have

$$(L_1 - \lambda I)^{-1} = \begin{pmatrix} \xi^{-1} & -\xi^{-1} r^\top \\ -\xi^{-1} r & -R + \xi^{-1} r r^\top \end{pmatrix},$$

where $r = (R_{11} + R_{1\,n-1}, R_{21} + R_{2\,n-1}, \ldots, R_{n-1\,1} + R_{n-1\,n-1})^\top$. This gives

$$M_1 = M_1(\lambda) = \left(\begin{array}{c|ccccc} m-1+w-\lambda-\frac{\delta_0\psi}{\xi} & -1-\frac{\delta_1\psi}{\xi} & -1-\frac{\delta_2\psi}{\xi} & \cdots & -1-\frac{\delta_{m-1}\psi}{\xi} \\ \hline -\mathbf{1}_{m-1} & & (1-\lambda)\, I & & \end{array}\right),$$

where $\psi = \psi(w, \lambda)$ is given by (6.11). Then, by virtue of Lemma A.0.2, we have

Lemma 6.2.9. For real $\lambda > 0$, assume $R = Q_{n-1}^{-1}$ exists, and $\xi(\delta, \lambda) \neq 0$. Then, $\lambda \neq 1$ is an eigenvalue of L_{G_p} if and only if

$$\lambda^2 - \left[m + w - \frac{\delta_0 \psi}{\xi}\right] \lambda + w - \frac{\delta \psi}{\xi} = 0, \tag{6.15}$$

or equivalently, one of the following holds:

$$\lambda = \frac{1}{2}\left(m + w - \sqrt{(m+w)^2 - 4w + \frac{4(\delta - \delta_0 \lambda)\psi}{\xi}}\right) \tag{6.16}$$

or

$$\lambda = \frac{1}{2}\left(m + w + \sqrt{(m+w)^2 - 4w + \frac{4(\delta - \delta_0 \lambda)\psi}{\xi}}\right).$$

Remark 6.2.10. If $\lambda \notin \{\beta_{m,w}^-, \beta_{m,w}^+\}$, then relation (6.15) can be derived from the equation $\xi - y\psi = 0$ (see (6.9)), and vice versa. In other words, if $\lambda \neq \beta_{m,w}^{\pm}$, then relation (6.15) does not give any further information about the eigenvalue λ other than what $P_2 = 0$ gives, where P_2 is given by (6.9). However, since P_2 is not defined at $\beta_{m,w}^{\pm}$ (because μ is not defined at these points), we still require (6.15) to analyze $\lambda = \beta^{\pm}(m, w)$.

6.3 Proof of Theorem B

Throughout this section, we assume that $w_0 = 1$ and $w_i = 0$, where $1 \leq i \leq n-1$. Moreover, we have that $\delta \geq \delta_0 \geq 0$. Note that, to adapt this proof for Theorem A, it is sufficient to assume $\delta = \delta_0$. We start with the following definition.

Definition 6.3.1. Recall Definition 5.1.1. Assume $\beta_{m,1}^- \notin \{\alpha_l : 0 \leq l \leq n\}$ and let $\kappa \geq 2$ be the even integer such that $\beta_{m,1}^- \in (\alpha_{\kappa-2}, \alpha_\kappa)$.

1. Define $J_{\beta^-} := (\alpha_{\kappa-2}, \alpha_\kappa)$.
2. Let $2 \leq l \leq n-2$ be even. We define
$$J_l = \begin{cases} (\alpha_{l-1}, \alpha_l), & \text{if } 2 \leq l < \kappa, \\ (\alpha_l, \alpha_{l+1}), & \text{if } \kappa \leq l \leq n-2. \end{cases}$$
3. Define $J_{\beta^+} := (\alpha_{n-1}, \infty)$.
4. For the sake of convenience, we define the set of indices $\mathcal{I} := \{\beta^-, \beta^+\} \cup \{l : 0 < l < n \text{ and } l \text{ is even}\}$.

Remark 6.3.2. Note that when $\kappa = 2$, there does not exists J_l for $2 \leq l < \kappa$.

Remark 6.3.3. *Notice that* $\beta^+_{m,1} > m \geq 4$*, and so* $\beta^+_{m,1} \in J_{\beta^+}$.

Considering eigenvalues with their multiplicities, the perturbed Laplacian L_{G_p} has $n + m$ eigenvalues. The next lemma describes where these $n + m$ eigenvalues are located.

Lemma 6.3.4. Let $\overline{\delta} \neq 0$ be an arbitrary perturbation that satisfies $\delta < \delta_0 \beta^+_{m,1}$. Then, all the $n+m$ eigenvalues of the perturbed Laplacian L_{G_p} of model II are real and given by the union of the following four disjoint groups (see also Remark 6.3.6).

1. L_{G_p} has $\lfloor \frac{n-1}{2} \rfloor + 1$ real eigenvalues given by $\{\alpha_l : \text{ where } 0 \leq l \leq n-1 \text{ and } l \text{ is even}\}$.
2. L_{G_p} has $m - 2$ of repeated eigenvalue $\lambda = 1$.
3. Recall the set $\mathcal{I}$. Each interval J_γ for $\gamma \in \mathcal{I}$ and $\gamma \neq \beta^+$ contains exactly one real eigenvalue of L_{G_p} (except possibly for the $m-2$ eigenvalues 1 counted in item (2)). We have $\lfloor \frac{n}{2} \rfloor$ of these intervals, and so L_{G_p} has $\lfloor \frac{n}{2} \rfloor$ real eigenvalues given by these intervals.
4. The interval J_{β^+} contains two real eigenvalues of the perturbed Laplacian L_{G_p}. Thus, L_{G_p} has 2 eigenvalues given by J_{β^+}.

Remark 6.3.5. Observe that $\left(\lfloor \frac{n-1}{2} \rfloor + 1\right) + (m-2) + \lfloor \frac{n}{2} \rfloor + 2 = n + m$.

Remark 6.3.6. The sets of the eigenvalues given by items (1) and (2) might not be disjoint, i.e. $\alpha_l = 1$ for some even l. The same may happen for (2) and (3), i.e. the eigenvalue in J_γ given by item (3) equals to 1. The eigenvalue 1 in such scenarios are counted separately from the $m-2$ eigenvalues 1 given in item (2). In such scenarios, the multiplicity of eigenvalue 1 is $m - 1$.

The proof of Lemma 6.3.4 is postponed to Section 6.3.1. We now prove Theorem B.

Part (1) of Theorem B follows from Theorem C which is proved later in Section 6.4. Here, we show that part (1) of Theorem B satisfies the corresponding assumptions of Theorem C. Recall S given by (5.4). Setting $w_0 = 1$ and $w_i = 0$, where $1 \leq i \leq n-1$,

gives

$$S = \frac{\alpha_2 \left[\delta \left(\alpha_2 - m\right) + \delta_0 - \delta\right]}{\left(\alpha_2 - \beta_{m,1}^-\right)\left(\alpha_2 - \beta_{m,1}^+\right)} \tag{6.17}$$

and

$$\sum_{i=0}^{n-1} w_i \cos\left(\frac{n}{2} - i\right)\theta = \cos\frac{n\theta}{2}, \qquad \text{where} \qquad \theta = \pi - \cos^{-1}\left(\frac{\beta_{m,1}^- - 2}{2}\right). \tag{6.18}$$

Take into account that $\delta_0 \leq \delta$ and $\alpha_2 < 4$. When $\alpha_2 < \beta_{m,1}^-$, we have $S < 0$. On the other hand, when $\alpha_1 < \beta_{m,1}^- < \alpha_2$, we have $\frac{\pi}{n} < \theta < \frac{2\pi}{n}$ and so $\cos\frac{n\theta}{2} < 0$, where θ is as above. Therefore, part (1a) of Theorem B follows from parts (1a) and (1e) of Theorem C, and part (1b) of Theorem B follows directly from part (1c) of Theorem C.

Part (2a) of Theorem B is a consequence of part (2a) of Theorem C, since, as mentioned above, when $\alpha_2 < \beta_{m,1}^-$, we have $S < 0$.

Let us now prove part (2b) of Theorem B. First, assume $\alpha_2 < \beta_{m,1}^-$. This implies $\kappa > 2$. Thus, by Lemma 6.3.4, L_{G_p} has a unique eigenvalue in the interval $J_2 = (\alpha_1, \alpha_2)$ which is indeed the spectral gap of L_{G_p}. Denote it by $\lambda_2\left(L_{G_p}\right)$. Since the spectral gap of the unperturbed Laplacian L_G is α_2, we have $\lambda_2\left(L_{G_p}\right) < \lambda_2\left(L_G\right)$. This shows that, in the case $\alpha_2 < \beta_{m,1}^-$, the statement of part (1a) of Theorem B holds for arbitrary perturbation $\overline{\delta}$ that satisfies $\delta < \delta_0\beta_{m,1}^+$.

Now, assume $\beta_{m,1}^- < \alpha_2$. This implies $\kappa = 2$, i.e. $J_{\beta^-} = (0, \alpha_2)$. According to Lemma 6.3.4, L_{G_p} has a unique eigenvalue in the interval $J_{\beta^-} = (0, \alpha_2)$ which is indeed the spectral gap of L_{G_p}. Denote it by $\lambda_2\left(\overline{\delta}\right)$. Note that the spectral gap of the unperturbed graph L_G is $\lambda_2\left(0\right) = \beta_{m,1}^-$. Following Lemma 6.2.9, we have

$$\lambda_2\left(\overline{\delta}\right) = \frac{1}{2}\left(m + 1 - \sqrt{\left(m+1\right)^2 - 4 + \frac{4\left[\delta - \delta_0\lambda_2\left(\overline{\delta}\right)\right]}{\xi}}\right), \tag{6.19}$$

where $\xi = \xi\left(\delta, \lambda_2\left(\overline{\delta}\right)\right) = \delta - 2\sin\theta\tan\frac{n\theta}{2}$ and $\theta = \pi - \cos^{-1}(\frac{\lambda_2\left(\overline{\delta}\right)-2}{2})$. Observe that when $\overline{\delta} = 0$ (and consequently, $\delta = \delta_0 = 0$), $\lambda_2\left(0\right) = \beta_{m,1}^-$ satisfies this relation. According to (6.19), the proof follows from this observation that for a given $\overline{\delta}$, we have $\lambda_2\left(\overline{\delta}\right) > \lambda_2\left(0\right)$, $\lambda_2\left(\overline{\delta}\right) = \lambda_2\left(0\right)$ and $\lambda_2\left(\overline{\delta}\right) < \lambda_2\left(0\right)$ if and only if the expression

$$\frac{\delta - \delta_0 \lambda_2\left(\overline{\delta}\right)}{\xi} \tag{6.20}$$

be negative, zero and positive, respectively.

First, consider the case $\alpha_1 < \lambda_2(0) = \beta^-_{m,1} < \alpha_2$. It is easily seen that $\beta^-_{m,1} \leq \beta^-_{4,1} \approx 0.21$ for all $m \geq 4$. Thus, having $\alpha_1 = 2\left(1 - \cos\frac{\pi}{n}\right) < \beta^-_{m,1} < 0.21$ yields $n \geq 7$ which implies $\alpha_2 = 2\left(1 - \cos\frac{2\pi}{n}\right) < 1$. Note also that as $\overline{\delta}$ changes, $\lambda_2\left(\overline{\delta}\right)$ remains in $(0, \alpha_2)$ (this is a consequence of part (3) of Lemma 6.3.4). Therefore

$$\delta - \delta_0 \lambda_2\left(\overline{\delta}\right) > \delta - \delta_0 + \delta_0\left[1 - \alpha_2\right] \geq \max\{\delta - \delta_0, \delta_0\left[1 - \alpha_2\right]\}. \tag{6.21}$$

Thus, the numerator of (6.20) is positive for any $\overline{\delta} \neq 0$. Regarding the denominator of (6.20), note that $\xi(0, \beta^-_{m,1}) > 0$ when $\alpha_1 < \beta^-_{m,1} < \alpha_2$. We claim that $\xi\left(\delta, \lambda_2\left(\overline{\delta}\right)\right) > 0$ for all $\overline{\delta}$. Taking into account that ξ is a smooth function of (δ, λ) for $\lambda \neq \alpha_1$, the claim will be proved once we show that $\lambda_2(\overline{\delta}) > \alpha_1$ holds for any $\overline{\delta}$ and also ξ does not vanish as $\overline{\delta}$ varies.

We first show that $\lambda_2(\overline{\delta}) > \alpha_1$ for all $\overline{\delta}$. Assume the contrary; there exists $\overline{\delta}^\dagger$ and correspondingly $\delta^\dagger$ and $\delta^\dagger_0$ for which $\lambda_2(\overline{\delta}^\dagger) = \alpha_1$. However, $\lim_{\delta \to \delta^\dagger} \xi = \infty$. On the other hand, the numerator of (6.20) converges to $\delta^\dagger - \delta^\dagger_0 \alpha_1 > 0$. Therefore, as $\delta \to \delta^\dagger$, expression (6.20) converges to zero which, by (6.19), implies that $\lambda_2(\overline{\delta}^\dagger) = \beta^-_{m,1}$ and so $\beta^-_{m,1} = \alpha_1$. This contradicts the assumption $\beta^-_{m,1} \notin \{\alpha_l : 0 \leq l < n\}$ of Theorem B. Thus, $\lambda_2(\overline{\delta}) < \alpha_1$ for all $\overline{\delta}$.

Since $\alpha_1 < \lambda_2(\overline{\delta}) < \alpha_2$ for all $\overline{\delta}$, we have that $\sin\theta \tan\frac{n\theta}{2} < 0$, where $\theta = \pi - \cos^{-1}(\frac{\lambda_2(\overline{\delta})-2}{2})$. This yields $\xi > \delta$ for all $\overline{\delta}$ which means that it cannot vanish as $\overline{\delta}$ varies. Therefore, the numerator and denominator of (6.20) are both positive. It then follows from (6.21), that when $\alpha_1 < \beta^-_{m,1} < \alpha_2$, we have $\lambda_2(L_{G_p}) < \lambda_2(L_G)$, as desired.

Now, we consider the case $0 < \lambda_2(0) = \beta^-_{m,1} < \alpha_1$. We first show that $\lambda_2(\overline{\delta}) < \alpha_1$ for all $\overline{\delta}$. Assume the contrary; there exists $\overline{\delta}^\dagger$ and correspondingly $\delta^\dagger$ and $\delta^\dagger_0$ for which $\lambda_2(\overline{\delta}^\dagger) = \alpha_1$. However, $\lim_{\delta \to \delta^\dagger} \xi = -\infty$. On the other hand the numerator of (6.20) converges to $\delta^\dagger - \delta^\dagger_0 \alpha_1 \geq 0$ (note that $\alpha_1 \leq 1$ for all $n \geq 3$). Therefore, as $\delta \to \delta^\dagger$,

expression (6.20) converges to zero which, by (6.19), implies that $\lambda_2(\overline{\delta}^\dagger) = \beta^-_{m,1}$ and so $\beta^-_{m,1} = \alpha_1$. This contradicts the assumption $\beta^-_{m,1} \notin \{\alpha_l : 0 \leq l < n\}$ of Theorem B. Thus, $\lambda_2(\overline{\delta}) < \alpha_1$ for all $\overline{\delta}$.

It is easily seen that $\xi(0, \beta^-_{m,1}) < 0$ when $0 < \beta^-_{m,1} < \alpha_1$. We claim that $\xi(0, \beta^-_{m,1}) < 0$ for all $\overline{\delta}$. Note that ξ is a smooth function for $\lambda \neq \alpha_1$. On the other hand, we have shown that $\lambda_2(\overline{\delta}) < \alpha_1$ for all $\overline{\delta}$. Thus, to prove the claim, we need to show that ξ does not vanish as $\overline{\delta}$ varies. Assume the contrary; there exists $\overline{\delta}^\dagger$ and correspondingly $\delta^\dagger$ and $\delta^\dagger_0$ such that as $\overline{\delta} \to \overline{\delta}^\dagger$, we have $\xi(\delta, \lambda_2(\overline{\delta}^\dagger)) \to 0$. By (6.19), this requires the numerator of (6.20) to vanish at $\overline{\delta}^\dagger$, i.e. $\delta^\dagger - \delta^\dagger_0 \lambda_2(\overline{\delta}^\dagger) = 0$. However, by $\lambda_2(\overline{\delta}) < \alpha_1$ and taking into account that $\alpha_1 \leq 1$ for all $n \geq 3$, we obtain

$$\delta^\dagger - \delta^\dagger_0 \lambda_2\left(\overline{\delta}^\dagger\right) \geq \max\left\{\delta^\dagger - \delta^\dagger_0, \delta^\dagger_0\left[1 - \lambda_2\left(\overline{\delta}^\dagger\right)\right]\right\} > 0. \tag{6.22}$$

This contradicts the assumption of vanishing ξ at $\overline{\delta}^\dagger$. Therefore, we have $\xi(0, \beta^-_{m,1}) < 0$ for all $\overline{\delta}$. It then follows from (6.21), that when $0 < \beta^-_{m,1} < \alpha_1$, we have $\lambda_2(L_{G_p}) > \lambda_2(L_G)$, as desired. This finishes the proof of part (2b) and the proof of Theorem B.

6.3.1 Proof of Lemma 6.3.4

So far, we have used Lemma 6.3.4 to prove Theorem B. We are now in the position of proving this lemma.

The proof of Lemma 6.3.4 is based on Lemma 6.2.7. In the setting of Theorems A and B, we assume $w_0 = 1$ and $w_i = 0$ for $i = 1, \ldots, n-1$. In this case, (6.12) is written as

$$p(\theta) = 2[\cos n\theta - 1] + [\delta - y] \cdot \frac{\sin n\theta}{\sin \theta}. \tag{6.23}$$

Then, Lemma 6.2.7 gives

Lemma 6.3.7. *For $0 \leq \lambda < 4$, let $\theta = \pi - \cos^{-1}(\frac{\lambda-2}{2})$. Consider p given by (6.23). Then*

1. *for even $0 \leq l \leq n-1$, we have $p(\frac{l\pi}{n}) = 0$.*
2. *for odd $1 \leq l \leq n-1$, we have $p(\frac{l\pi}{n}) = -4$.*

3. for even $1 \leq l \leq n-1$, we have

$$p'\left(\frac{l\pi}{n}\right) = \frac{n}{\sin\frac{l\pi}{n}}\left[\delta - y\right] = \frac{-n\lambda}{\sin\frac{l\pi}{n}} \cdot \frac{(m-\lambda)\,\delta + \delta - \delta_0}{\lambda^2 - (m+1)\,\lambda + 1}. \tag{6.24}$$

Proof of part (1) of Lemma 6.3.4. The proof directly follows from part (1) of Lemma 6.3.7. □

Proof of part (2) of Lemma 6.3.4. The proof directly follows from Lemma 6.2.3 and its proof. □

Proof of part (3) of Lemma 6.3.4. We first investigate $p'\left(\frac{l\pi}{n}\right)$ given by (6.24). The expression $\lambda^2 - (m+1)\,\lambda + 1$ is positive if and only if $\lambda < \beta^-_{m,1}$ or $\lambda > \beta^+_{m,1} > 4$. For $\lambda = 2[1 - \cos\frac{l\pi}{n}]$, when l is even, this gives

$$\begin{cases} \lambda^2 - (m+1)\,\lambda + 1 > 0, & \text{if } l \text{ is even and } 2 \leq l < \kappa, \\ \lambda^2 - (m+1)\,\lambda + 1 < 0, & \text{if } l \text{ is even and } \kappa \leq l < n-1. \end{cases}$$

When $\lambda \in J_\gamma$, for $\gamma \neq \beta^+$, we have that $\lambda < 4 \leq m$. On the other hand, $\delta_0 \leq \delta$. This implies that when $\delta > 0$, we have $(m-\lambda)\,\delta + \delta - \delta_0 > 0$. Taking into account that $\sin\frac{l\pi}{n} > 0$ for all $0 \leq l \leq n-1$, we obtain

$$\begin{cases} p'\left(\frac{l\pi}{n}\right) < 0, & \text{if } l \text{ is even and } 2 \leq l < \kappa, \\ p'\left(\frac{l\pi}{n}\right) > 0, & \text{if } l \text{ is even and } \kappa \leq l < n-1. \end{cases}$$

We have that $p'\left(\frac{l\pi}{n}\right) = 0$ if and only if $\delta = 0$. This, together with item (1) of Lemma 6.3.7, gives

Proposition 6.3.8. Any point of $\{\alpha_l : \text{ where } 0 \leq l \leq n-1 \text{ and } l \text{ is even}\}$ is a multiple eigenvalue of L_G with multiplicity 2, and a simple eigenvalue of L_{G_p}.

For even l, when $2 \leq l < \kappa$, we have $p'\left(\frac{l\pi}{n}\right) < 0$. This means that $p\,(\theta)$ is positive for θ close to $\frac{l\pi}{n}$ and $\theta < \frac{l\pi}{n}$. On the other hand, $p\left(\frac{(l-1)\pi}{n}\right) = -4 < 0$. Thus, by the intermediate value theorem, the function p has a root in the interval $\left(\frac{(l-1)\pi}{n}, \frac{l\pi}{n}\right)$. This implies that L_{G_p} has a real eigenvalue in J_l. Analogously, for even l and when $\kappa \leq l < n-1$, the function p has a root in the interval $\left(\frac{l\pi}{n}, \frac{(l+1)\pi}{n}\right)$ which means that L_{G_p} has a real eigenvalue in J_l.

At $\overline{\delta} = 0$ (when there is no perturbation), the interval J_{β^-} has the eigenvalue $\beta^-_{m,1}$. As $\overline{\delta}$ changes, the eigenvalue $\beta^-_{m,1}$ starts to move. However, since $\alpha_{\kappa-2}$ and α_κ are simple roots, this eigenvalue cannot leave the interval $J_{\beta^-} = (\alpha_{\kappa-2}, \alpha_\kappa)$. This means that L_{G_p} has a real root in J_{β^-}.

We have shown that each interval J_γ for $\gamma \in \mathcal{I}$ and $\gamma \neq \beta^+$ contains at least one real eigenvalue of L_{G_p}. To finish the proof, we need to show that each of these intervals has exactly one eigenvalue (apart from $m-2$ eigenvalues 1 counted in item (2) that might be located in one of these intervals). Note that, we have already counted $n+m-2 = \lfloor \frac{n-1}{2} \rfloor + 1 + m - 2 + \lfloor \frac{n}{2} \rfloor$ real eigenvalues of L_{G_p}. The matrix L_{G_p} has $n+m$ eigenvalues. Thus, the proof of part (3) of this lemma is done after we prove part (4) of this lemma below. □

Proof. [Proof of part (4) of Lemma 6.3.4] So far, we have shown that the matrix L_{G_p} has at least $n+m-2$ eigenvalues located outside of the interval J_{β^+}, and as $\overline{\delta}$ varies, none of these eigenvalues enters this interval. Notice that for arbitrary $\delta > 0$, when n is even, $p(\frac{(n-1)\pi}{n}) < 0$, and when n is odd, $p(\frac{(n-1)\pi}{n}) = 0$ and $p'(\frac{(n-1)\pi}{n}) \neq 0$. This means that if there is any real eigenvalue located in J_{β^+}, then it cannot leave this interval as $\overline{\delta}$ changes. As shown below, for sufficiently small $\overline{\delta} \neq 0$, the interval J_{β^+} has exactly two real eigenvalues. On the other hand, L_{G_p} is a real matrix. Therefore, if it possesses non-real eigenvalues, then they need to appear as pairs (complex conjugates). This means that, for a given $\overline{\delta}$, we either have two real eigenvalues in J_{β^+} or none. Therefore, the proof of part (4) of Lemma 6.3.4 is done if we show that, under the condition $\delta < \delta_0 \beta^+_{m,1}$, the interval J_{β^+} has at least one real eigenvalue.

First, we show that when $\overline{\delta} \neq 0$ is sufficiently small, the interval J_{β^+} has exactly two real eigenvalues. For even n, this is obvious since at $\delta = 0$, we have two eigenvalues $\lambda = 4$ and $\lambda = \beta^+_{m,1}$, and so, as $\overline{\delta}$ varies and remains sufficiently small, these two eigenvalues might move but they remain in J_{β^+} and do not collide (so, they remain real). The case of odd n is similar; since for $\overline{\delta} \neq 0$, we have $p'(\alpha_{n-1}) > 0$ and $p(-4) < 0$, the intermediate value theorem implies that there is a root in the interval $(\alpha_{n-1}, 4)$. On the other hand, the eigenvalue $\beta^+_{m,1} \in (4, \infty)$ of L_G might

move as $\overline{\delta}$ varies but as far as $\overline{\delta}$ is sufficiently small, it does not collied with the eigenvalue that we just found in the interval $(\alpha_{n-1}, 4)$. Therefore, we have that for small $\overline{\delta} \neq 0$, the interval J_{β^+} contains exactly two real eigenvalues of L_{G_p}.

We now prove that J_{β^+} has at least one real root when $\delta < \delta_0 \beta^+_{m,1}$. Evaluating (6.9) at $\lambda > 4$, gives

$$P_2(\lambda) = (-1)^{n-1} \cdot \frac{\sinh n\theta}{\sinh \theta} \left[\frac{2 \sinh \theta}{\sinh n\theta} \cdot [(-1)^n - \cosh n\theta] + \delta - \frac{\delta - \delta_0 \lambda}{\lambda^2 - (m+1)\lambda + 1} \right],$$

where $\theta = \cosh^{-1}(\frac{\lambda - 2}{2})$. Note that $\lambda^2 - (m+1)\lambda + 1$ vanishes at $\lambda = \beta^{\pm}_{m,1}$. Thus, when $\delta < \delta_0 \beta^+_{m,1}$, we have

$$\lim P_2(\lambda) = \begin{cases} +\infty, & \text{for even } n, \text{ as } \lambda \to \left(\beta^+_{m,1}\right)^-, \\ -\infty, & \text{for odd } n, \text{ as } \lambda \to \left(\beta^+_{m,1}\right)^-. \end{cases} \tag{6.25}$$

When n is even, we have $P_2(4) = \frac{4n[(m-3)\delta - \delta_0]}{13 - 4m} < 0$. Taking (6.25) and the fact that P_2 is smooth on $(\alpha_{n-1}, \beta^+_{m,1})$ into account (see Lemma 6.2.5), the intermediate value theorem implies the existence of a real root of P_2 in $(4, \beta^+_{m,1}) \subset J_{\beta^+}$, as desired.

For the case of odd n, we have $p(\frac{(n-1)\pi}{n}) = 0$ and $p'(\frac{(n-1)\pi}{n}) > 0$. Thus, for $\lambda > \alpha_{n-1}$ and close to α_{n-1}, we have $P_2(\lambda) > 0$. Taking (6.25) and the fact that P_2 is smooth on $(\alpha_{n-1}, \beta^+_{m,1})$ into account (see Lemma 6.2.5), the intermediate value theorem implies the existence of a real root of P_2 in $(\alpha_{n-1}, \beta^+_{m,1}) \subset J_{\beta^+}$, as desired. This ends the proof. □

6.4 Proof of Theorem C

6.4.1 Proof of part (1) of Theorem C

We first prove that for sufficiently small $\overline{\delta}$, all the eigenvalues of L_{G_p} are real. It is known that the roots of a polynomial (in our case, the characteristic polynomial of L_{G_p}) depends continuously on the coefficients of that polynomial. Therefore, if $\{\lambda_i(\overline{\delta}) : i = 1, \ldots, n+m\}$ is the spectrum of L_{G_p}, then $\lambda_i(\overline{\delta})$ is a continuous function of $\overline{\delta}$. It is a direct consequence of the implicit function theorem that if $\lambda_i(0)$ is a simple eigenvalue of L_G, then for sufficiently small $\overline{\delta}$, we have that $\lambda_i(\overline{\delta})$ is real. Thus, to prove our statement, we need to investigate how multiple eigenvalues of the unperturbed Laplacian L_G behaves as $\overline{\delta}$ varies.

Recall Proposition 5.2.3. According to Remark 5.2.4 and the assumption $\beta^-_{m,w} \notin \{\alpha_l : 0 \leq l < n\}$ of the theorem, we have that $\beta^-_{m,w}$ and $\beta^+_{m,w}$ are simple eigenvalues of L_G. Note that $1 \in \{\alpha_l : 0 \leq l \leq n, \text{ and } l \text{ is even}\}$ if and only if $\frac{n}{6}$ is an integer. First, assume $\frac{n}{6} \notin \mathbb{Z}$. In this case, the multiplicity of all the eigenvalues α_l except for 0 and 4 (the eigenvalue 4 appears only when n is even) is 2. However, it follows from Lemma 6.2.7 that, for each even l, as $\overline{\delta}$ varies, one of the two eigenvalues α_l remains as an eigenvalue of L_{G_p} for small arbitrary $\overline{\delta}$, and the other eigenvalue moves continuously. This means that from each of the multiple eigenvalues α_l, two real eigenvalues get born. On the other hand, following Lemma 6.2.3 and its proof, the eigenvalue 1 remains an eigenvalue of L_{G_p} with multiplicity $m-2$. This implies that when $\frac{n}{6} \notin \mathbb{Z}$ and $\overline{\delta}$ is sufficiently small, all the eigenvalues of L_{G_p} are real. The case of $\frac{n}{6} \in \mathbb{Z}$ is similar. With the same conclusion, except for $l = \frac{n}{6}$, i.e. $\alpha_l = 1$, two real eigenvalues get born from each eigenvalue α_l, where $l = 1, \ldots, n-1$. Regarding $\alpha_l = 1$ (note that the multiplicity of 1 as an eigenvalue of L_G in this case is m), we have that $\alpha_l = 1$ remains an eigenvalue of L_{G_p} with multiplicity $m-1$ and a new real eigenvalue gets born from it. This proves that when $\overline{\delta}$ is sufficiently small, all the eigenvalues of L_{G_p} are real.

The rest of the proof of part (1) of Theorem C is based on the following lemma

Lemma 6.4.1. *Consider p and S given by (6.12) and (5.4), respectively. We have*

1. *The expressions S and $p'\left(\frac{2\pi}{n}\right)$ have the same sign.*
2. *Assume $\alpha_2 < \beta^-_{m,w}$. Then, for any arbitrary $\overline{\delta}$, we have $p\left(\frac{\pi}{n}\right) < 0$.*
3. *For sufficiently small $\overline{\delta}$, we have $p\left(\frac{3\pi}{n}\right) < 0$.*

Proof. The first part follows from the relation $p'\left(\frac{2\pi}{n}\right) = \frac{n}{\sin\frac{2\pi}{n}} S$ (see relation (6.13)). For the other two parts, note that by Lemma 6.2.7 and for odd $1 \leq l \leq n-1$, we have $p(\frac{l\pi}{n}) = -4 - \frac{2y}{\sin\frac{l\pi}{n}} \sum_{i=0}^{n-1} w_i \sin\frac{il\pi}{n}$. Regarding the case $l = 1$, assumption $\alpha_2 < \beta^-_{m,w}$ implies that $\alpha_2 < 1$ (see Remark 5.2.4) and therefore $\alpha_1 < 1$. Thus, $\delta - \delta_0\alpha_1 > 0$, and therefore, $y = y(\alpha_1) = \frac{\delta - \delta_0\alpha_1}{\alpha_1^2 - (m+w)\alpha_1 + w} > 0$. On the other hand, $\sin\frac{i\pi}{n} \geq 0$ for $i = 0, \ldots, n-1$ and so $\sum_{i=0}^{n-1} w_i \sin\frac{il\pi}{n} \geq 0$. This implies $p\left(\frac{\pi}{n}\right) < 0$ for any $\overline{\delta}$.

The proof of the last part follows from $\left|\frac{2y}{\sin\frac{3\pi}{n}}\sum_{i=0}^{n-1} w_i \sin\frac{3i\pi}{n}\right| \ll 4$ which holds when $\overline{\delta}$ is small enough. □

Proof of parts (1a) and (1b) of Theorem C. Since $\alpha_2 < \beta^-_{m,w}$, the spectral gap of L_G is α_2. It follows from Lemma 6.2.7 that $p\left(\frac{2\pi}{n}\right) = 0$ for all $\overline{\delta}$. On the other hand, $p\left(\frac{\pi}{n}\right)$ and $p\left(\frac{3\pi}{n}\right)$ are both negative for sufficiently small $\overline{\delta}$. Therefore, by intermediate value theorem, the eigenvalue that gets born from α_2 as $\overline{\delta}$ varies is located in the interval (α_2, α_3) if $p'\left(\frac{2\pi}{n}\right) > 0$, and is located in (α_1, α_2) if $p'\left(\frac{2\pi}{n}\right) < 0$. On the other hand, by part (1) of Lemma 6.4.1, we have that $p'\left(\frac{2\pi}{n}\right)$ and S have the same sign. This proves parts (1a) and (1b) of Theorem C. □

Proof of parts (1c), (1d) and (1e) of Theorem C. Since $\beta^-_{m,w} < \alpha_2$, the spectral gap of L_G is $\beta^-_{m,w}$. So, we need to see how $\beta^-_{m,w}\left(\overline{\delta}\right)$ changes as $\overline{\delta}$ varies. By (6.16), for sufficiently small $\overline{\delta} \neq 0$, we have that $\beta^-_{m,w}\left(\overline{\delta}\right) > \beta^-_{m,w}$ if $\frac{\left(\delta-\delta_0\beta^-_{m,w}\right)\psi}{\xi} < 0$, and $\beta^-_{m,w}\left(\overline{\delta}\right) < \beta^-_{m,w}$ if $\frac{\left(\delta-\delta_0\beta^-_{m,w}\right)\psi}{\xi} > 0$. Note that, $\delta - \delta_0\beta^-_{m,w} > 0$, since $\delta \geq \delta_0$ and $\beta^-_{m,w} < 1$. Thus, all we need to do is to investigate the sign of $\frac{\psi\left(\overline{w},\beta^-_{m,w}\right)}{\xi\left(\delta,\beta^-_{m,w}\right)}$.

Note that $\xi\left(\delta,\beta^-_{m,w}\right)$ and $\xi\left(0,\beta^-_{m,w}\right)$ have the same sign provided that $\overline{\delta}$ is sufficiently small and $\xi\left(0,\beta^-_{m,w}\right) \neq 0$. Following Lemma 6.2.6, $\xi\left(0,\beta^-_{m,w}\right) = -2\sin\theta\tan\frac{n\theta}{2}$, where $\theta = \pi - \cos^{-1}(\frac{\beta^-_{m,w}-2}{2})$. It is easily seen that $\xi\left(0,\beta^-_{m,w}\right) < 0$ if $0 < \beta^-_{m,w} < \alpha_1$, and $\xi\left(0,\beta^-_{m,w}\right) > 0$ if $\alpha_1 < \beta^-_{m,w} < \alpha_2$. On the other hand, by Lemma 6.2.6,

$$\psi\left(\overline{w},\beta^-_{m,w}\right) = \frac{1}{\cos\frac{n\theta}{2}}\sum_{i=0}^{n-1} w_i \cos\left(\frac{n}{2}-i\right)\theta,$$

where $\theta = \pi - \cos^{-1}(\frac{\beta^-_{m,w}-2}{2})$. Note that $\cos\frac{n\theta}{2} < 0$ if $\alpha_1 < \beta^-_{m,w} < \alpha_2$, and $\cos\frac{n\theta}{2} > 0$ if $0 < \beta^-_{m,w} < \alpha_1$. Moreover, when $0 < \beta^-_{m,w} < \alpha_1$, we have that $\cos\left(\frac{n}{2}-i\right)\theta > 0$ for $i = 0, \ldots, n-1$, and therefore $\sum_{i=0}^{n-1} w_i \cos\left(\frac{n}{2}-i\right)\theta > 0$. We have

$$\begin{cases} \frac{\psi\left(\overline{w},\beta^-_{m,w}\right)}{\xi\left(0,\beta^-_{m,w}\right)} < 0 & \text{if } 0 < \beta^-_{m,w} < \alpha_1, \\ \frac{\psi\left(\overline{w},\beta^-_{m,w}\right)}{\xi\left(0,\beta^-_{m,w}\right)} > 0 & \text{if } \alpha_1 < \beta^-_{m,w} < \alpha_2, \text{ and } \sum_{i=0}^{n-1} w_i \cos\left(\frac{n}{2}-i\right)\theta < 0, \\ \frac{\psi\left(\overline{w},\beta^-_{m,w}\right)}{\xi\left(0,\beta^-_{m,w}\right)} < 0 & \text{if } \alpha_1 < \beta^-_{m,w} < \alpha_2, \text{ and } \sum_{i=0}^{n-1} w_i \cos\left(\frac{n}{2}-i\right)\theta > 0. \end{cases}$$

This ends the proof of parts (1c), (1d) and (1e) of Theorem C. □

Proof of part (2) of Theorem C. Since $\alpha_2 < \beta^-_{m,w}$, we have $\lambda_2(L_G) = \alpha_2$ (see Proposition 5.2.3). On the other hand, by Lemma 6.4.1, S and $p'\left(\frac{2\pi}{n}\right)$ have the same sign. If $S < 0$, since $p\left(\frac{\pi}{n}\right) < 0$ (see Lemma 6.4.1), the intermediate value theorem implies that L_{G_p} has an eigenvalue (p has a root) smaller than α_2. Denote this eigenvalue by $\lambda\left(\overline{\delta}\right)$. When the perturbation is small, this eigenvalue is indeed the spectral gap of L_{G_p}, as discussed in the proof of part (1a). However, for large perturbation, there is the possibility of the emergence of non-real eigenvalues of L_{G_p}. In such a scenario, there might be complex conjugates eigenvalues of L_{G_p} whose real part decreases and becomes smaller than $\lambda\left(\overline{\delta}\right)$. This means that the spectral gap is not necessarily a real number, however, since $\lambda\left(\overline{\delta}\right) < \alpha_2$, we always have $\mathrm{Re}\left(\lambda_2\left(L_{G_p}\right)\right) < \lambda_2(L_G)$. This proves part (2a) of the theorem.

The proof of part (2a) is similar. For small perturbations, as discussed in the proof of part (1b) of the theorem, we have that $\lambda_2\left(L_{G_p}\right) = \alpha_2$. In fact, α_2 is an eigenvalue of L_{G_p} for arbitrary $\overline{\delta}$. However, as we discussed above, there is a possibility of the emergence of non-real eigenvalues for L_{G_p} when the perturbation $\overline{\delta}$ is large. Thus, this might be the case that the real parts of these non-real eigenvalues reduce, and they become the spectral gap of L_{G_p}. In any case, the property $\mathrm{Re}\left(\lambda_2\left(L_{G_p}\right)\right) \leq \lambda_2(L_G)$ always holds. This proves part (2b) of the theorem. □

7. CONCLUSION

7.1 Informal Statements of Our Results

We consider three models, namely model I, II, and III, illustrated in Figures 7.1, 7.2, and 7.3, respectively. These three models have a master-slave structure. Indeed, the unperturbed graph in all these models consists of a cycle graph C_n, a star graph S_m, and cutset edge(s) starting from the cycle and ending at the hub of the star. We perturb these networks and break the master-slave structure by adding directed link(s) from the star to the cycle (red-color edges in the figures).

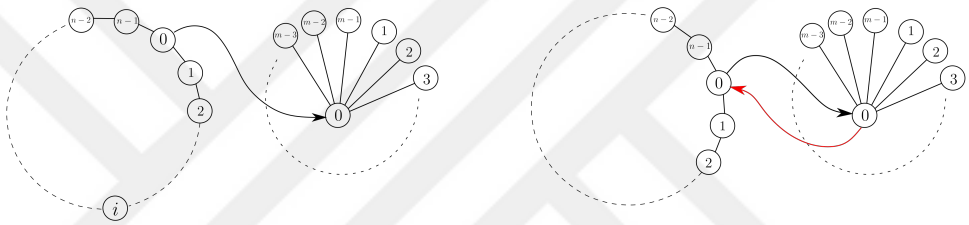

(a) The unperturbed graph G. (b) The perturbed graph G_p.

Figure 7.1: Model I: Breaking the master-slave through hub coupling. We add a directed link from the hub of the star to the cutset node (the red-color edge) where the cutset node refers to the node which cutset edge starts from. The weakly connected directed graph becomes the strongly connected directed graph consequent to the perturbation shown by the red arrow.

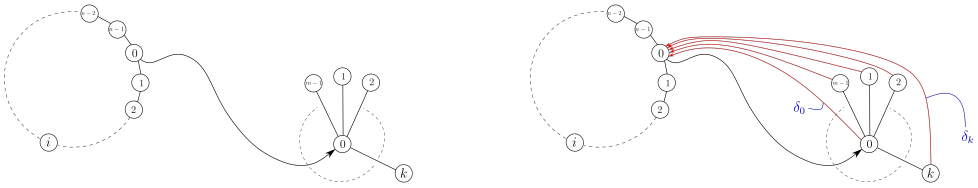

(a) The unperturbed graph G. (b) The perturbed graph G_p.

Figure 7.2: Model II: Breaking the master-slave through multiple couplings. We add links from some nodes of the star to the cutset node of the cycle.

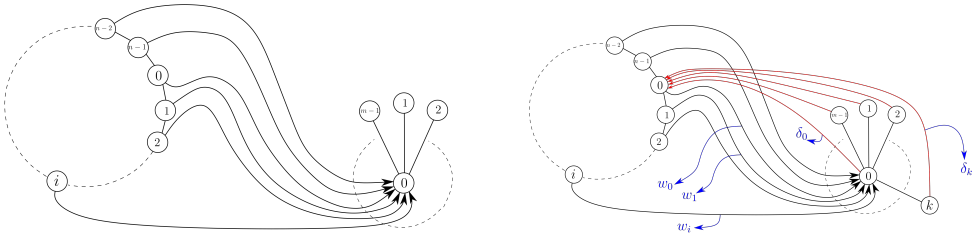

(a) The unperturbed graph G. (b) The perturbed graph G_p.

Figure 7.3: Model III: Breaking the generalized master-slave through multiple couplings. We add links from some nodes of the star to the one cutset node of the cycle where multiple cutset nodes exist.

We define the adjacency matrix of G by $A_G = (A_{ij})$, where $A_{ij} \geq 0$ is the weight of the directed edge starting from node j and ending at node i. We define the Laplacian matrix of G by $L_G := D_G - A_G$, where D_G is a diagonal matrix whose (i,i)-entry is the in-degrees of the node i of G.

Let L_G and L_{G_p} represent the Laplacians of the unperturbed and perturbed graphs of each of these models, respectively. Let $\lambda_2(L_G)$ and $\lambda_2(L_{G_p})$ be the associated spectral gaps. Our results explain how the perturbation affects the spectral gap of the Laplacian matrices of these models. Assume $\delta_0 \geq 0$ is the weight of the perturbation edge starting from the hub and $\delta \geq 0$ is the sum of the weights of all the perturbation edges. In model I, we have $\delta_0 = \delta$, and in the other two models, $\delta_0 \leq \delta$.

All these models are discussed precisely in previous sections. Here, we rather give an informal version of our main results.

Theorem A'. [Informal statement] Consider model I illustrated in Figure 7.1. Let the perturbation $\delta > 0$ be arbitrary (it does not need to be sufficiently small). We have

1. Although L_{G_p} is not necessarily symmetric, all of its eigenvalues are real.
2. Let m and n be the sizes of the star and cycle, respectively. There exists a critical $m_c = m_c(n)$ (for large m and n, it is estimated by $m_c \approx \frac{n^2}{\pi^2} - 1$) such that $\lambda_2\left(L_{G_p}\right) < \lambda_2\left(L_G\right)$ if and only if $m \leq m_c$.

Theorem B'. [Informal statement] Consider model II illustrated in Figure 7.2. We have

1. Under a local perturbation, the statement of Theorem A' is valid for model II as well. Indeed, when $\delta > 0$ is sufficiently small, all the eigenvalues of L_{G_p} are real and, the perturbation decreases the spectral gap if and only if the size of the star is smaller than the critical value $m_c(n)$.

2. Let $\rho := \frac{\delta_0}{\delta}$. This ratio can be seen as a measure for the perturbation that the cycle receives from the hub of the star relative to the perturbation it receives from the leaves of the star. We have $\rho \leq 1$, and by setting $\rho = 1$, the model II reduces to model I. Under a global perturbation (δ be arbitrary), we prove that not only the statement of Theorem A' is valid for model II when $\rho = 1$ but also it is valid when $\rho > K$, where $0 < K < 1$ is a constant given in Section 5.

3. According to the previous item, under a global perturbation, if $\rho > K$ holds, all the eigenvalues of L_{G_p} are real. Non-real eigenvalues may appear when this condition fails. However, we can still prove that, for perturbations of arbitrary size (whether or not $\rho > K$ holds), we have $\mathrm{Re}\left(\lambda_2\left(L_{G_p}\right)\right) < \lambda_2\left(L_G\right)$ if the size of the star is smaller than a critical value $m_c(n)$ (this critical value is different from the previous one and for large m and n it is estimated by $m_c \approx \frac{n^2}{4\pi^2} - 1$).

Theorem C'. [Informal statement] Consider model III illustrated in Figure 7.3. We have

1. Under a local perturbation, all the eigenvalues of L_{G_p} are real. When $\lambda_2(L_G) = \lambda_2(L_{C_n})$, i.e., $\lambda_2(L_G)$ belongs to the upper left block of L_G, the spectral gap decreases or does not change after perturbation. These two characteristic behaviors can be classified using the parity of the function S given in equation (5.4), the arguments of which depend on the sizes of cycle and star, the total and individual weights of cutset edges, the topology of cutset (which nodes of the cycle are connected to the star), and the sizes of the perturbation δ and δ_0. On the other hand, when $\lambda_2(L_G) = \lambda_2(L_{S_{m+D_C}})$, the decrease of the

spectral gap due to the perturbation occurs if $\lambda_2(L_{S_{m+D_C}})$ is in the interval between the spectral gap of a path with size n and the spectral gap of a cycle with size n and if the summation in 1e, whose arguments depend on the sizes of cycle and star, the topology of cutset, the total and individual weights of cutset edges, has odd parity.

2. Under a global perturbation and when $\lambda_2(L_G) = \lambda_2(L_{C_n})$, the real part of the spectral gap decreases or strictly decreases after perturbation depending on the parity of the function S given in equation (5.4).

7.2 Discussions

In this research, we have investigated the effect of link modifications on network synchronization and have revealed the emergent synchronization loss due to link additions. Even though the existence of such cases is proved by Poignard et al. (Poignard, Pade and Pereira, 2019, pp. 1919-1942), there was a lack of rigorous prescription to detect when link additions hinder the synchronization depending on the graph parameters.

We presented a classification scheme depending on the underlying graph parameters. Despite the fact that this research only includes some motifs, it examines not only sufficiently small perturbations but it also includes wide range of perturbations for all sized networks and discovers different settings. Thus, one can predict rigorously for particular settings when the synchronization loss occurs due to link additions via this study. Since cycle and star are fundamental motifs in many networks, this research might provide a basis for future generalizations.

BIBLIOGRAPHY

Agaev, R. and Chebotarev, P. (2006) 'The matrix of maximum out forests of a digraph and its applications', *arXiv preprint* math/0602059, p1424–1450.

Bondy, J. A. and Murty, U. S. R. (1976) *Graph theory with applications*. (Vol. 290). London: Macmillan.

Braess, D. (1968) 'Über ein Paradoxon aus der Verkehrsplanung', *Unternehmensforschung*, 12(1), p258-268.

Brouwer, A. E. and Haemers, W. H. (2011) *Spectra of graphs*. Newyork: Springer Science and Business Media.

Chebotarev, P. and Agaev, R. (2013) 'Matrices of forests, analysis of networks, and ranking problems', *Procedia Computer Science*, 17, p1134–1141.

Eldan, R., Rácz, M. Z. and Schramm, T. (2017) 'Braess's paradox for the spectral gap in random graphs and delocalization of eigenvectors', *Random Structures Algorithms*, 50(4), p584–611.

Ermentrout, B. and Terman, D. H. (2010) *Mathematical foundations of neuroscience*. Vol. 35, New York: Springer.

Eroglu, D., Lamb, J. S. W. and Pereira, T. (2017) 'Synchronisation of chaos and its applications', *Contemporary Physics*, 58(3), p207–243.

Hart, J. D., Pade, J. P., Pereira, T., Murphy, T. E. and Roy, R. (2015) 'Adding connections can hinder network synchronization of time-delayed oscillators', *Physical Review E*, 92(2), p022804.

Hirsch, M. W., Smale, S. and Devaney, R. L. (2012) *Differential equations, dynamical systems, and an introduction to chaos*. Cambridge: Academic Press.

Horn, R. A. and Johnson, C. R. (2012) *Matrix analysis*. Newyork: Cambridge University Press.

Hu, G. Y. and O'Connell, R. F. (1996) 'Analytical inversion of symmetric tridiagonal matrices', *Journal of Physics A: Mathematical and General*, 29(7), p1511.

Meyer, C. D. (2000) *Matrix analysis and applied linear algebra*. Vol. 71, Philadelphia: SIAM.

Newman, M. (2018) *Networks*. Oxford: Oxford University Press.

Nishikawa, T. and Motter, A. E. (2010) 'Network synchronization landscape reveals compensatory structures, quantization, and the positive effect of negative interactions', *Proceedings of the National Academy of Sciences*, 107(23), p10342–10347.

Pade, J. P. and Pereira, T. (2015) 'Improving network structure can lead to functional failures', *Scientific reports*, 5(1), p1–6.

Pereira, T. (2011) 'Stability of Synchronized motion in complex networks', *arXiv preprint* arXiv:1112.2297, p1-47.

Pereira, T., Eldering, J., Rasmussen, M. and Veneziani, A. (2014) 'Towards a theory for diffusive coupling functions allowing persistent synchronization', *Nonlinearity*, 27(3), p501-525.

Pikovsky, A., Rosenblum, M. and Kurths, J. (2001) *A universal concept in nonlinear sciences*. Self, 2, 3.

Poignard, C., Pade, J. P. and Pereira, T. (2019) 'The effects of structural perturbations on the synchronizability of diffusive networks', *Journal of Nonlinear Science*, 29(5), p1919–1942.

Tucker, W. (1999) 'The Lorenz attractor exists', *Comptes Rendus de l'Académie des Sciences-Series I-Mathematics*, 328(12), p1197–1202.

Veerman, J. J. P. and Lyons, R. (2020) 'A primer on Laplacian dynamics in directed graphs', *arXiv preprint* arXiv:2002. 02605.

West, D. B. (2001) *Introduction to graph theory*. Upper Saddle River: Prentice Hall.

Wiggins, S. and Golubitsky, M. (2003) *Introduction to applied nonlinear dynamical systems and chaos*. New York: Springer.

APPENDIX A: TECHNICAL LEMMAS

Lemma A.0.1. Consider the block matrix $\begin{pmatrix} A & B \\ C & D \end{pmatrix}$ and assume D is invertible. Define $E := A - BD^{-1}C$. Then

1. $\det \begin{pmatrix} A & B \\ C & D \end{pmatrix} = \det(D) \times \det(E)$.
2. Assume E is invertible. Then, $\begin{pmatrix} A & B \\ C & D \end{pmatrix}^{-1} = \begin{pmatrix} E^{-1} & -E^{-1}BD^{-1} \\ -D^{-1}CE^{-1} & D^{-1} + D^{-1}CE^{-1}BD^{-1} \end{pmatrix}$.

Proof. See, e.g. (Meyer, 2000, p. 475) □

Lemma A.0.2. For $m \geq 4$, let X_0, X_1,..., X_{m-1} be real-valued functions defined on a subset of $\mathbb{R}$, and consider the $m \times m$ matrix

$$M = M(\lambda) = \left(\begin{array}{c|ccccc} m - \lambda + X_0(\lambda) & -1 + X_1(\lambda) & -1 + X_2(\lambda) & \cdots & -1 + X_{m-1}(\lambda) \\ \hline \mathbf{1}_{m-1} & & (1-\lambda)\,\mathrm{I} & & \end{array} \right).$$

Let $\lambda_0 \in \mathbb{R}$, and assume that all the functions X_i are defined at λ_0.

1. There exists $0 \neq v \in \mathbb{R}^m$ such that $M(\lambda_0)v = 0$ if and only if $\lambda_0 = 1$ or $\lambda = \lambda_0$ satisfies
$$\lambda^2 - [1 + m + X_0(\lambda)]\,\lambda + 1 + \sum_{i=0}^{m-1} X_i(\lambda) = 0. \tag{A.1}$$
2. Assume that there exists $1 \leq i \leq m-1$ such that $X_i(1) \neq 1$. Then, the vector subspace $E^{\text{right}} \subset \mathbb{R}^m$ (resp. $E^{\text{left}} \subset \mathbb{R}^m$) of all the solutions v of the equation $M(1)v = 0$ (resp. $v^\top M(1) = 0$) has $m-2$ dimensions.
3. Let $v = (v_0, v_1, \ldots, v_{m-1}) \in \mathbb{R}^m$. Then, any $v \in E^{\text{right}}$ satisfies the property $v_0 = 0$. Moreover, if there exists $1 \leq i \leq m-1$ such that $X_i(1) \neq 1$, then, any $v \in E^{\text{left}}$ satisfies the property $v_0 = 0$ too.

Proof. For $v = (v_0, v_1, \ldots, v_{m-1}) \in \mathbb{R}^m$, we have $M(\lambda)v = 0$ if and only if

$$[m - \lambda + X_0(\lambda)]\,v_0 + \textstyle\sum_{i=1}^{m-1} [-1 + X_i(\lambda)]\,v_i = 0, \quad \text{and} \tag{A.2}$$

$$v_0 + (1-\lambda)\,v_i = 0, \quad \text{for all } 1 \leq i \leq m-1. \tag{A.3}$$

This implies that for $\lambda = 1$, the equation $M(1)v = 0$ has a solution v if and only if $v \in E^{\text{right}}$ for

$$E^{\text{right}} := \{v \in \mathbb{R}^m | \quad v_0 = 0 \text{ and } \langle (v_1, v_2, \cdots, v_{m-1}), (X_1(1) - 1, \ldots, X_{m-1}(1) - 1) \rangle = 0\}, \tag{A.4}$$

where $\langle \cdot, \cdot \rangle$ is the standard Euclidean inner product in $\mathbb{R}^{m-1}$.

If $M(1)v = 0$, for $\lambda \neq 1$, has a solution v, then it follows from (A.3) that $v_0 \neq 0$ and $v_i = \frac{v_0}{1-\lambda}$, for all $1 \leq i \leq m-1$. Substituting this into (A.2), and multiplying the derived equation by $1 - \lambda$ give (A.1). This proves part (1).

Part (2) follows from (A.4). To prove part (3), let $v \in E^{\text{left}}$. By $v^\top M(1) = 0$, we have that if there exists $1 \leq i \leq m-1$ such that $X_i(1) \neq 1$, then $v_0 = 0$ and $v_1 + v_2 + \cdots + v_{m-1} = 0$. The set of all vs satisfying these properties is a $(m-2)$-dimensional subspace of $\mathbb{R}^m$. This finishes the proof of the lemma. □

CURRICULUM VITAE

Personal Information
Name and surname: Narçiçeği Kıran

Academic Background
Bachelor's Degree Education: Yıldız Technical University, Department of Physics
Post Graduate Education: Mimar Sinan University, Department of Physics, M. Sc.
Foreign Languages: English, German

Work Experience
Institutions Served and Their Dates:
Teaching Assistant, Altınbaş University, 03.2020-09.2020.
Researcher, Kadir Has University, 09.2020-06.2022.